CRA2017 (Oct. 10, 2017@Gadalajara)

Sub- & multi-TeV cosmic ray anisotropy and Tibet Air shower experiment

Kaz Munakata (Shinshu Univ.)

On behalf of The Tibet ASγ collaboration

SHINSHU UNIVERSITY

- Brief review of **sidereal diurnal anisotropy observed in 0.1~100 TeV** region.

- Cosmic ray shadow of the Sun **(Sun shadow) observed by Tibet III**.
  - ✓ **Possible influence of ICME on the shadow.**
  - ✓ **North-south displacement of the shadow and the IMF strength.**

The Tibet ASγ Collaboration

M.Amenomori(a), X.J.Bi(b), D.Chen(c), T.L.Chen(d), W.Y.Chen(b), S.W.Cui(e), Danzengluobu(d), L.K.Ding(b), C.F.Feng(f), Zhaoyang Feng(b), Z.Y.Feng(g), Q.B.Gou(b), Y.Q.Guo(b), H.H.He(b), Z.T.He(e), K.Hibino(h), N.Hotta(i), HaibingHu(d), H.B.Hu(b), J.Huang(b), H.Y.Jia(g), L.Jiang(b), F.Kajino(j), K.Kasahara(k), Y.Katayose(l), C.Kato(m), K.Kawata(n), M.Kozai(o,m), Labaciren(d), G.M.Le(p), A.F.Li(q,f,b), H.J.Li(d), W.J.Li(b,g), C.Liu(b), J.S.Liu(b), M.Y.Liu(d), H.Lu(b), X.R.Meng(d), T.Miyazaki(m), K.Mizutani(k,r), K.Munakata(m), T.Nakajima(m), Y.Nakamura(m), H.Nanjo(a), M.Nishizawa(s), T.Niwa(m), M.Ohnishi(n), I.Ohta(t), S.Ozawa(k), X.L.Qian(f,b), X.B.Qu(u), T.Saito(v), T.Y.Saito(w), M.Sakata(j), T.K.Sako(x,n), J.Shao(b,f), M.Shibata(l), A.Shiomi(y), T.Shirai(h), H.Sugimoto(z), M.Takita(n), Y.H.Tan(b), N.Tateyama(h), S.Torii(k), H.Tsuchiya(A), S.Udo(h), H.Wang(b), H.R.Wu(b), L.Xue(f), Y.Yamamoto(j), K.Yamauchi(l), Z.Yang(b), A.F.Yuan(d), T.Yuda(n), L.M.Zhai(c), H.M.Zhang(b), J.L.Zhang(b), X.Y.Zhang(f), Y.Zhang(b), YiZhang(b), Ying Zhang(b), Zhaxisangzhu(d) and X.X.Zhou(g)

(a)Department of Physics, Hirosaki Univ., Japan
(b)Key Laboratory of Particle Astrophysics, IHEP, CAS, China
(c)National Astronomical Observatories, CAS, China
(d)Department of Mathematics and Physics, Tibet Univ., China
(e)Department of Physics, Hebei Normal Univ., China
(f)Department of Physics, Shandong Univ., China
(g)Institute of Modern Physics, SouthWest Jiaotong Univ., China
(h)Faculty of Engineering, Kanagawa Univ., Japan
(i)Faculty of Education, Utsunomiya Univ., Japan
(j)Department of Physics, Konan Univ., Japan
(k)Research Institute for Science and Engineering, Waseda Univ., Japan
(l)Faculty of Engineering, Yokohama National Univ., Japan
(m)Department of Physics, Shinshu Univ., Japan
(n)ICRR, The Univ. of Tokyo, Japan
(o)ISAS/JAXA, Japan
(p)National Center for Space Weather, China Meteorological Administration, China
(q)School of Information Science and Engineering, Shandong Agriculture Univ., China
(r)Saitama Univ., Japan
(s)National Institute of Informatics, Japan
(t)Sakushin Gakuin Univ., Japan
(u)College of Science, China Univ. of Petroleum, China
(v)Tokyo Metropolitan College of Industrial Technology, Japan
(w)Max-Planck-Institut fur Physik, Deutschland
(x)Escuela de Ciencias Fisicas Nanotechnologia, Yachay Tech, Ecuador
(y)College of Industrial Technology, Nihon Univ., Japan
(z)Shonan Institute of Technology, Japan
(A)Japan Atomic Energy Agency, Japan

Sidereal diurnal anisotropy of Sub- & multi-TeV cosmic rays observed by UG-μ & AS detectors

Sidereal diurnal anisotropy of CRs

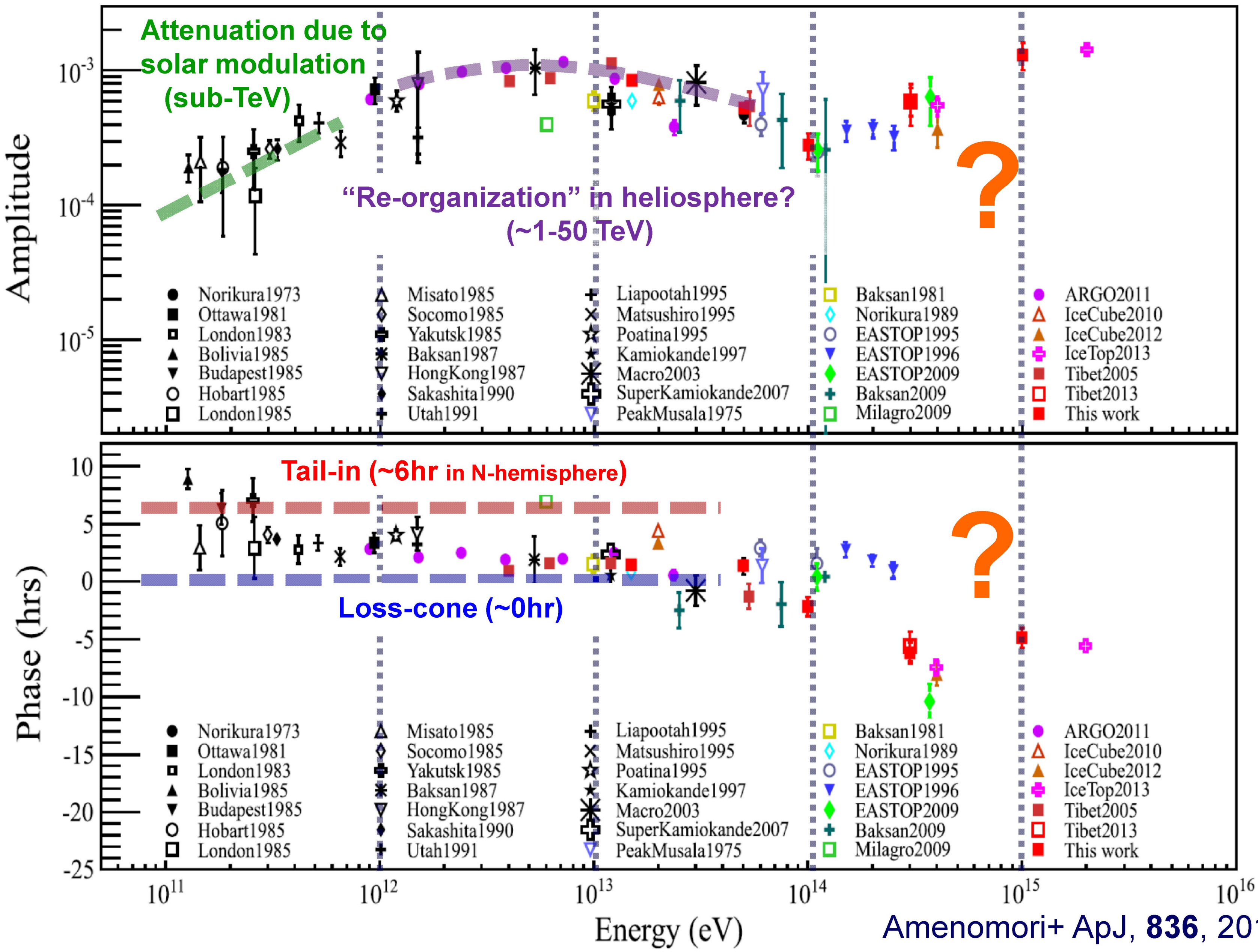

Amenomori+ ApJ, **836**, 2017

Solar Diurnal Anisotropy (DA)

Long term variation of Solar DA

2002 (solar Max.)

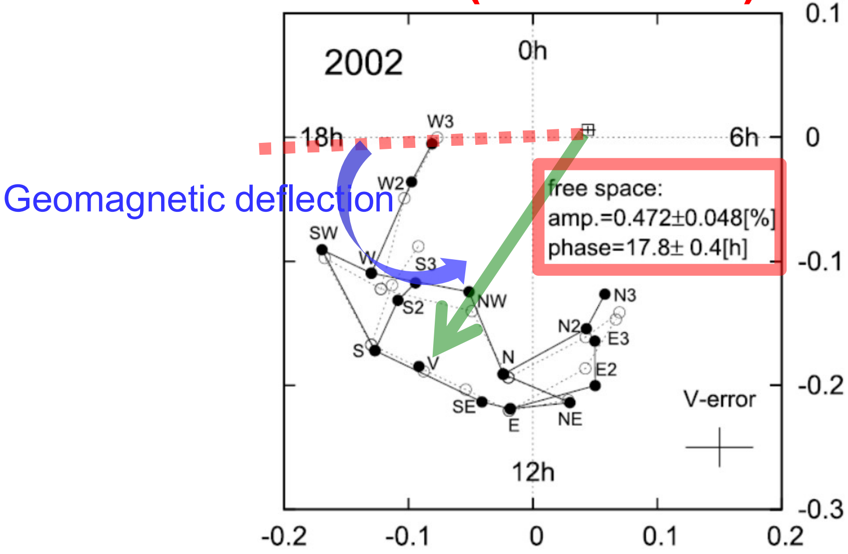

1976 (solar min. : A>0)

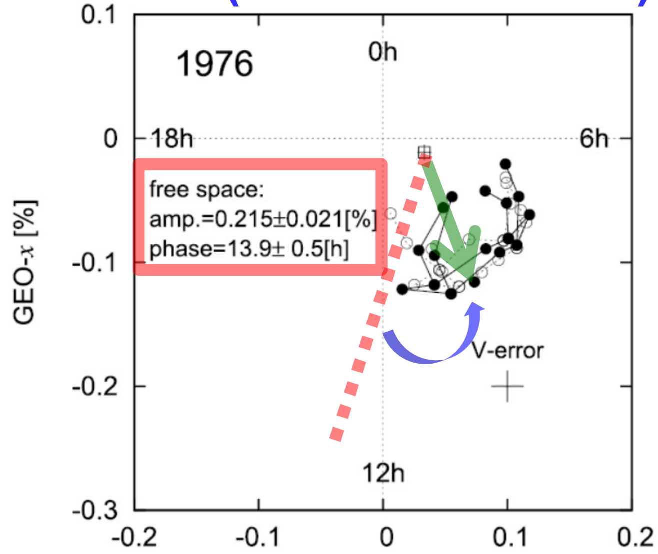

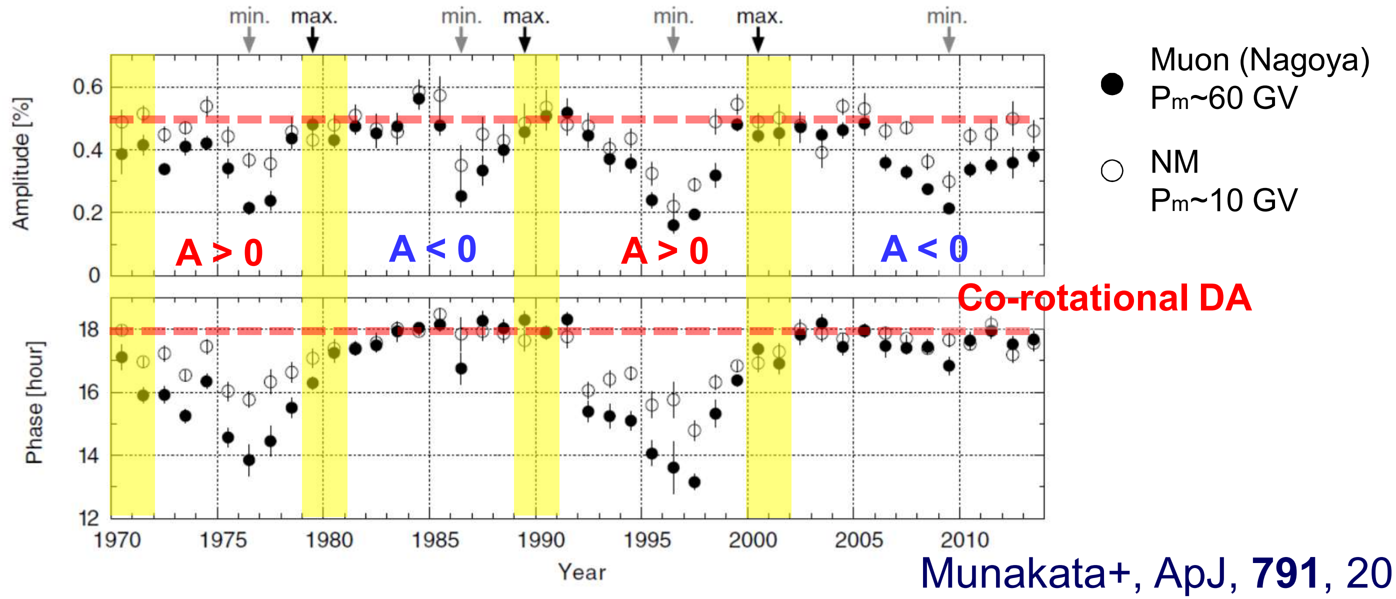

Munakata+, ApJ, **791**, 2014

Energy dependence of Solar & Sidereal DAs

solar：365 cycle/year
sidereal：366 cycle/year

Detector	Viewing lat.	Rock depth. (mwe)	Pm (GV)	operation
Nagoya-V	28°N	0	60	1970-
Misato-V	29°N	34	145	1974-
Sakashita-V	32°N	80	331	1978-1999
Matsushiro-V	37°N	220	659	1985-
Liapootah-V	36°S	154	519	1993-2005

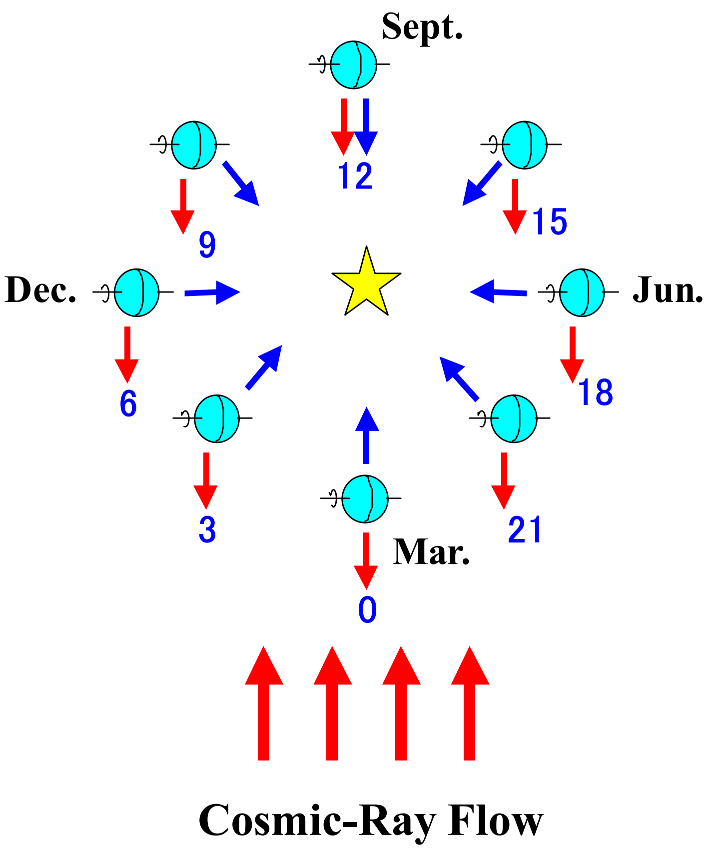

"Transparent" heliosphere

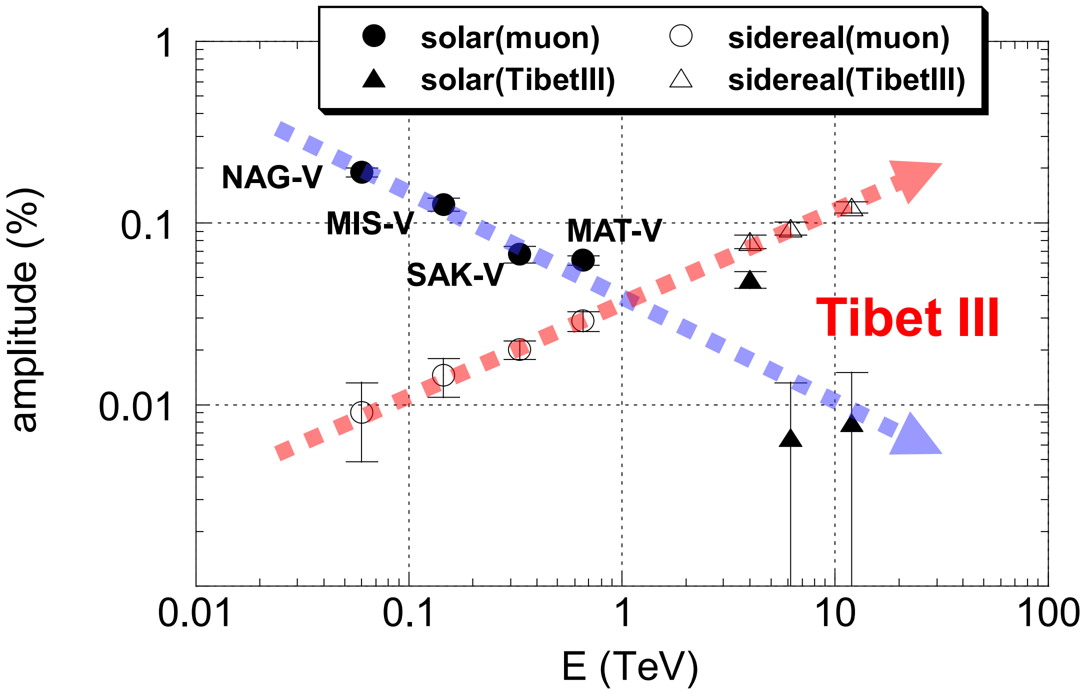

W. I. Axford

(Planetary and Space Sci., **13**, 1965)

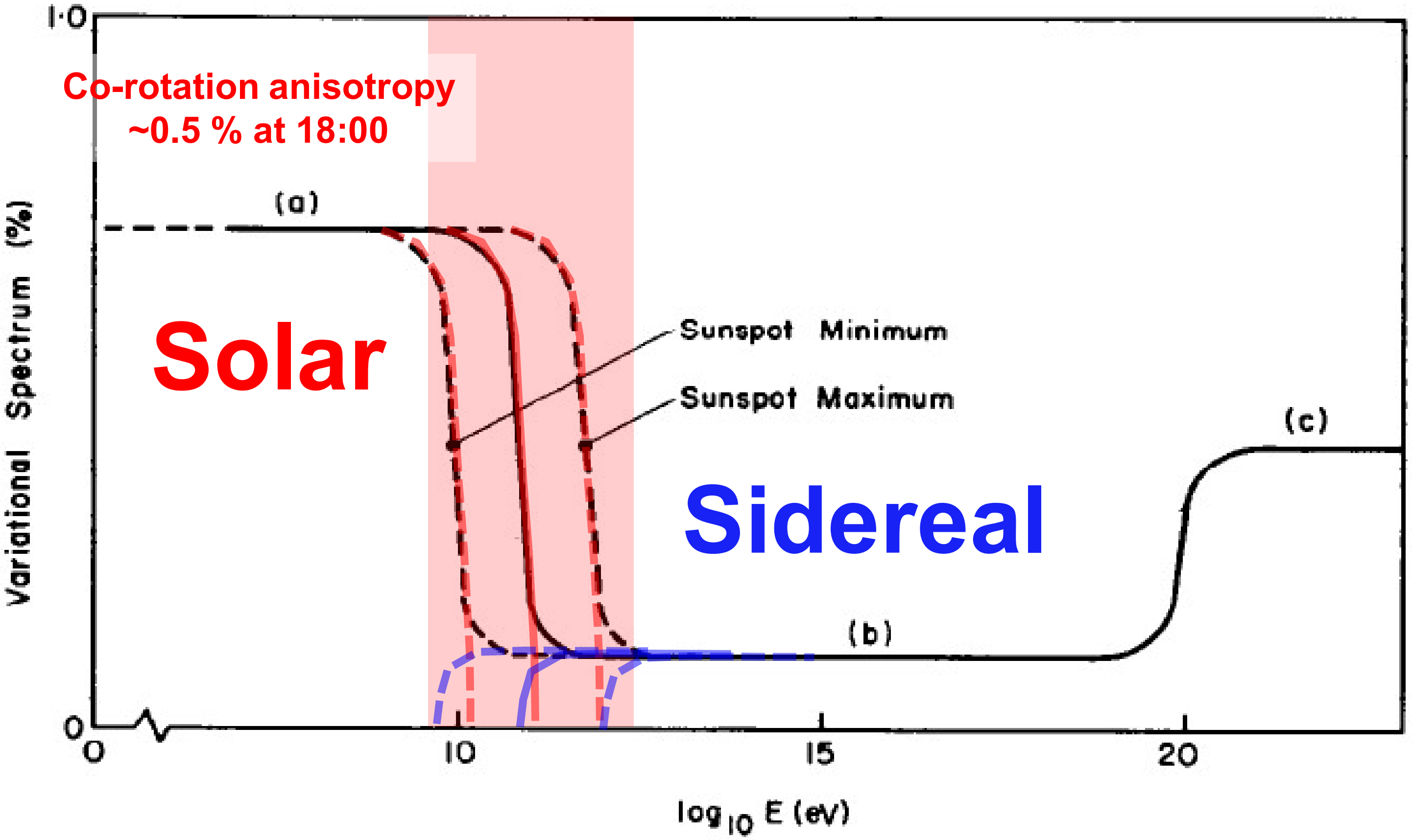

FIG. 6. SUGGESTED VARIATIONAL SPECTRUM OF THE DIURNAL MODULATION OF THE COSMIC RAY INTENSITY AT THE EARTH.

(a) REPRESENTS THE SOLAR DIURNAL VARIATION DUE TO CO-ROTATION OF THE COSMIC RAY GAS WITH THE SUN.

(b) REPRESENTS THE SIDEREAL DIURNAL VARIATION ASSOCIATED WITH STREAMING OF COSMIC RAYS WITHIN THE GALAXY, AND (c) THE SIDEREAL VARIATION DUE TO EXTRAGALACTIC EFFECTS. THE TRANSITION FROM (a) TO (b) VARIES THROUGH THE SUNSPOT CYCLE MORE OR LESS AS INDICATED.

Two Hemisphere Observations

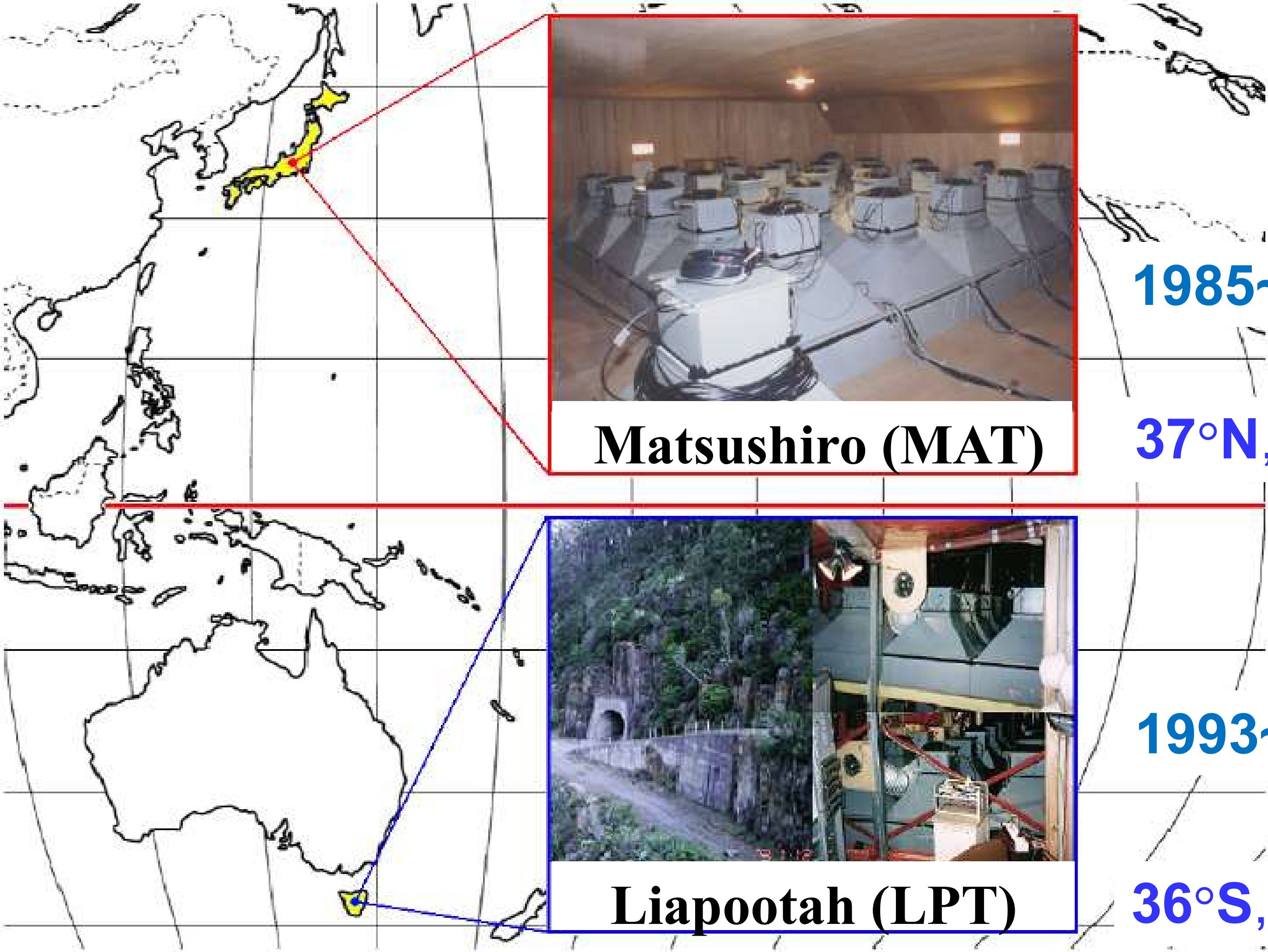

1985~present

37°N, 659GV

1993~2005

36°S, 519GV

THO of Sidereal DA (NS asymmetry)

Summation dial of sidereal DA

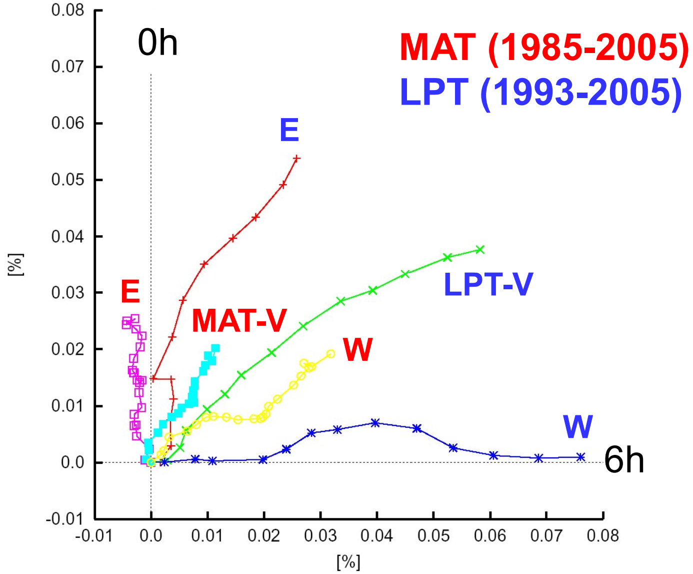

MAT (1985-2005)

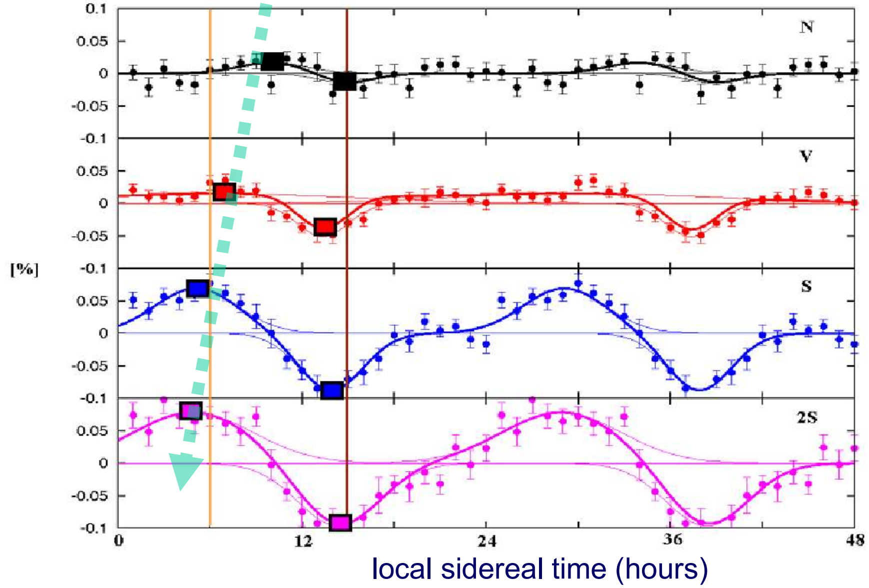

Percent anisotropy at 500 GV

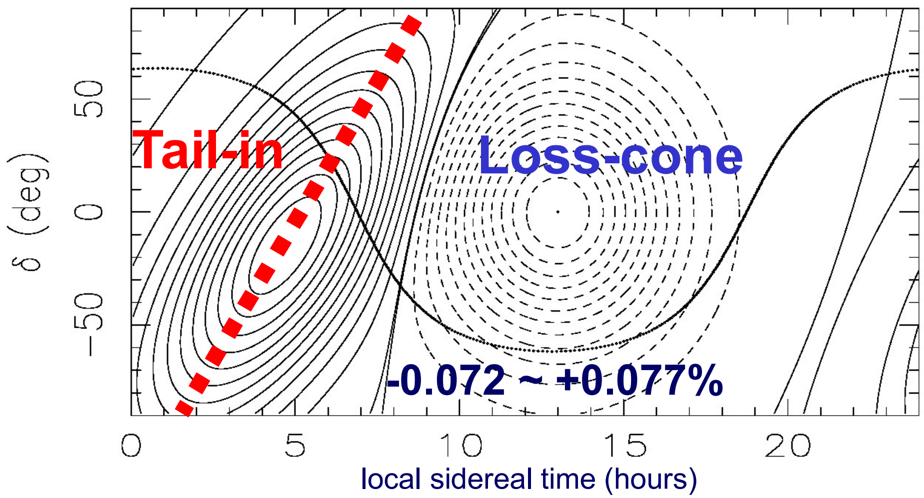

LPT (1993-2005)

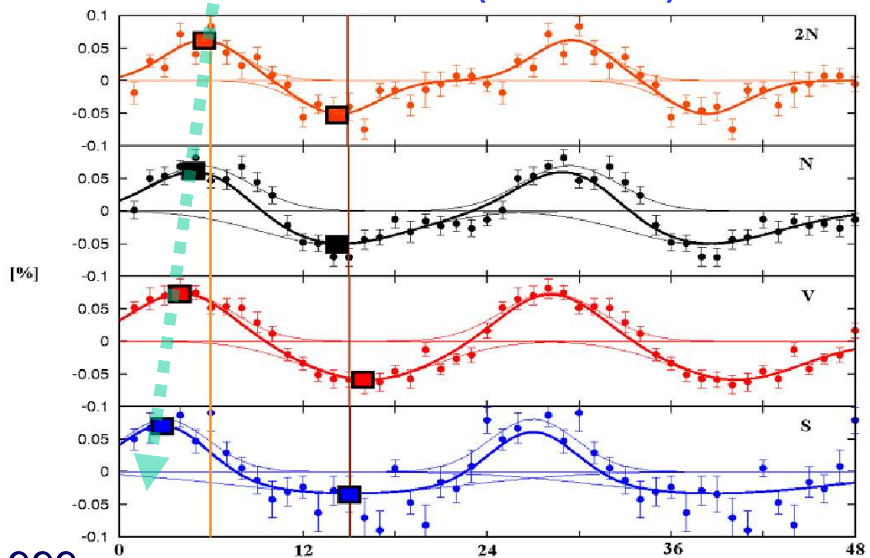

Hall+, JGR, **104**, 1999

Sky maps by THO & Tibet-III

by Tibet III (5°x5° pixel)

Amenomori+, Science, **314**, 2006

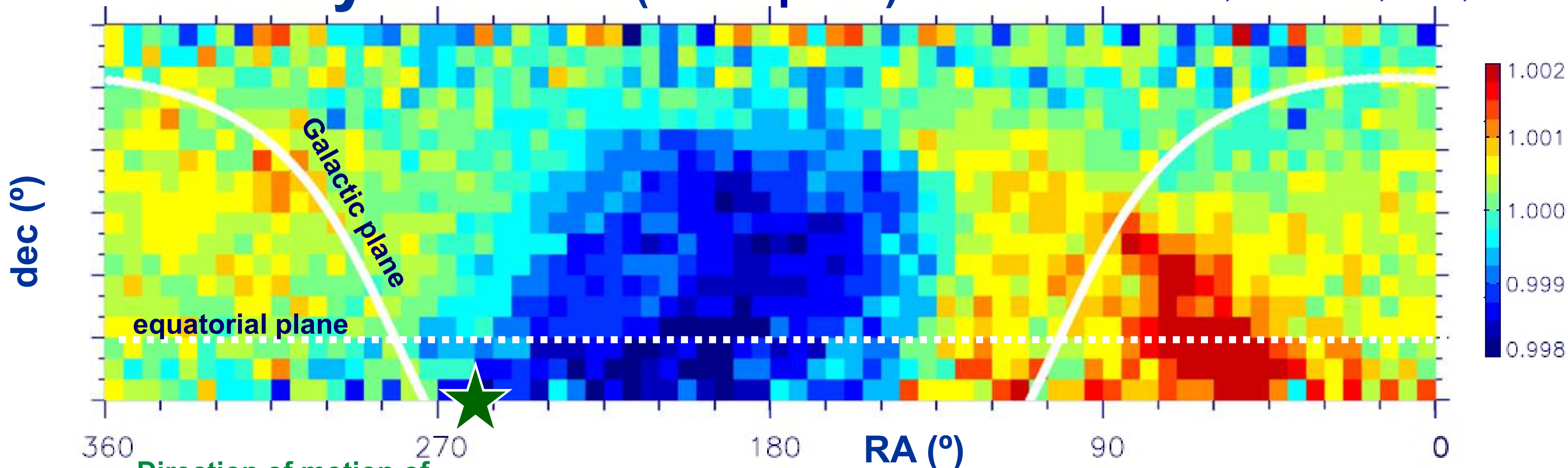

Direction of motion of
the heliosphere relative to LISM

by THO (white countour)

Hall+, JGR, **104**, 1998

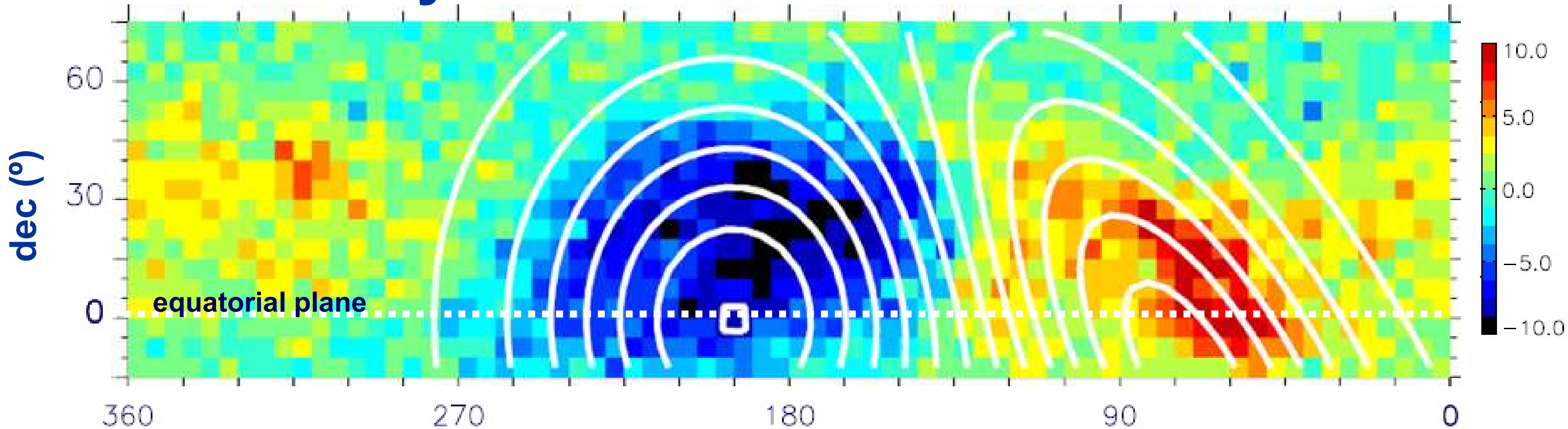

Solar cycle variation of DA
(observation by MAT in 1985-2008 @~500 GV)

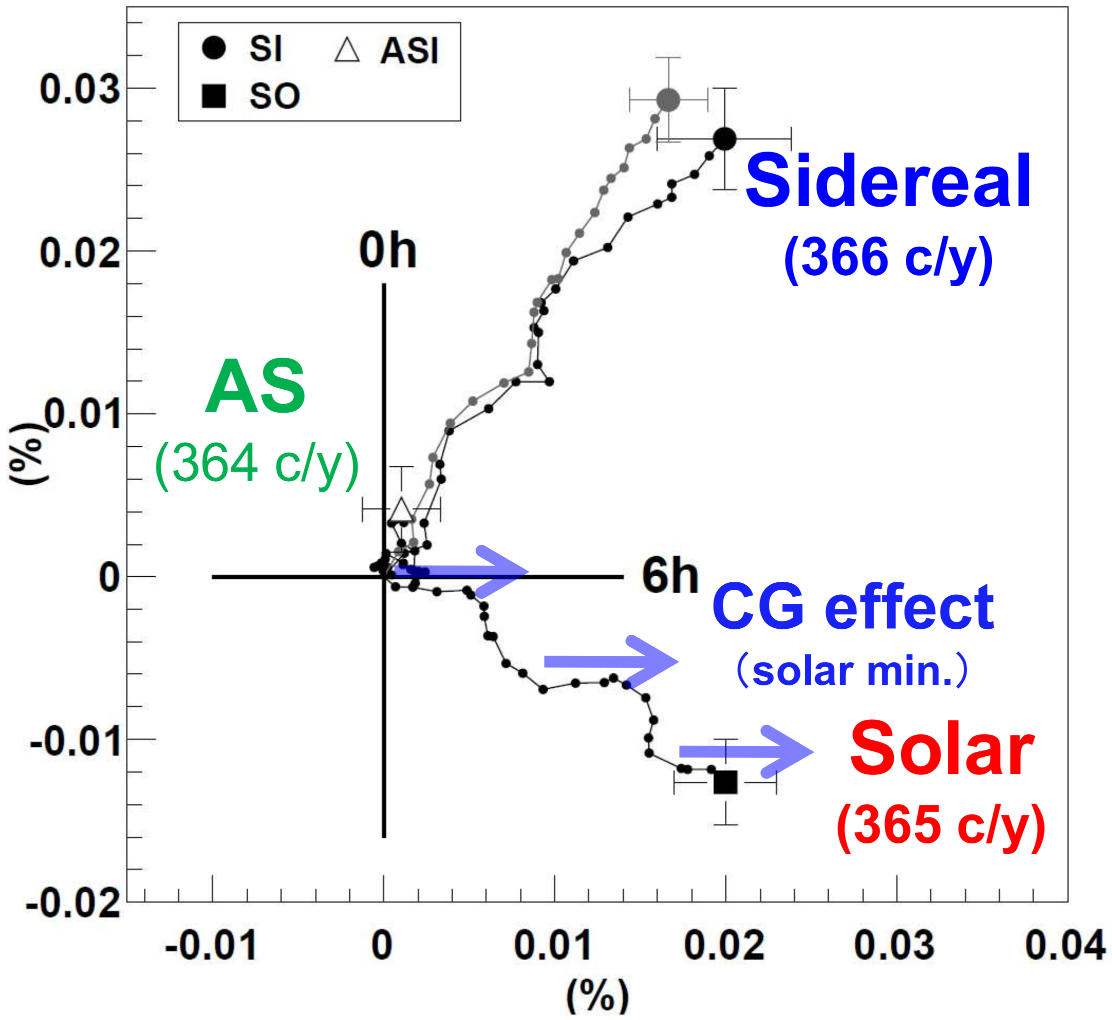

Solar DA

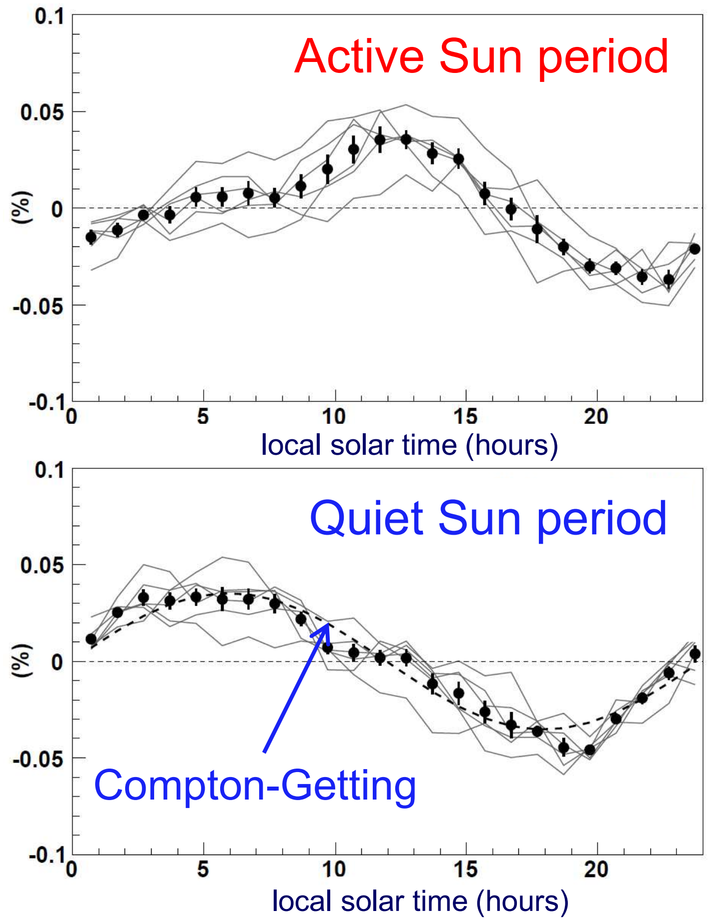

Munakata+, ApJ, **712**, 2010

Solar activity

Solar
(CG-subtracted)

Sidereal

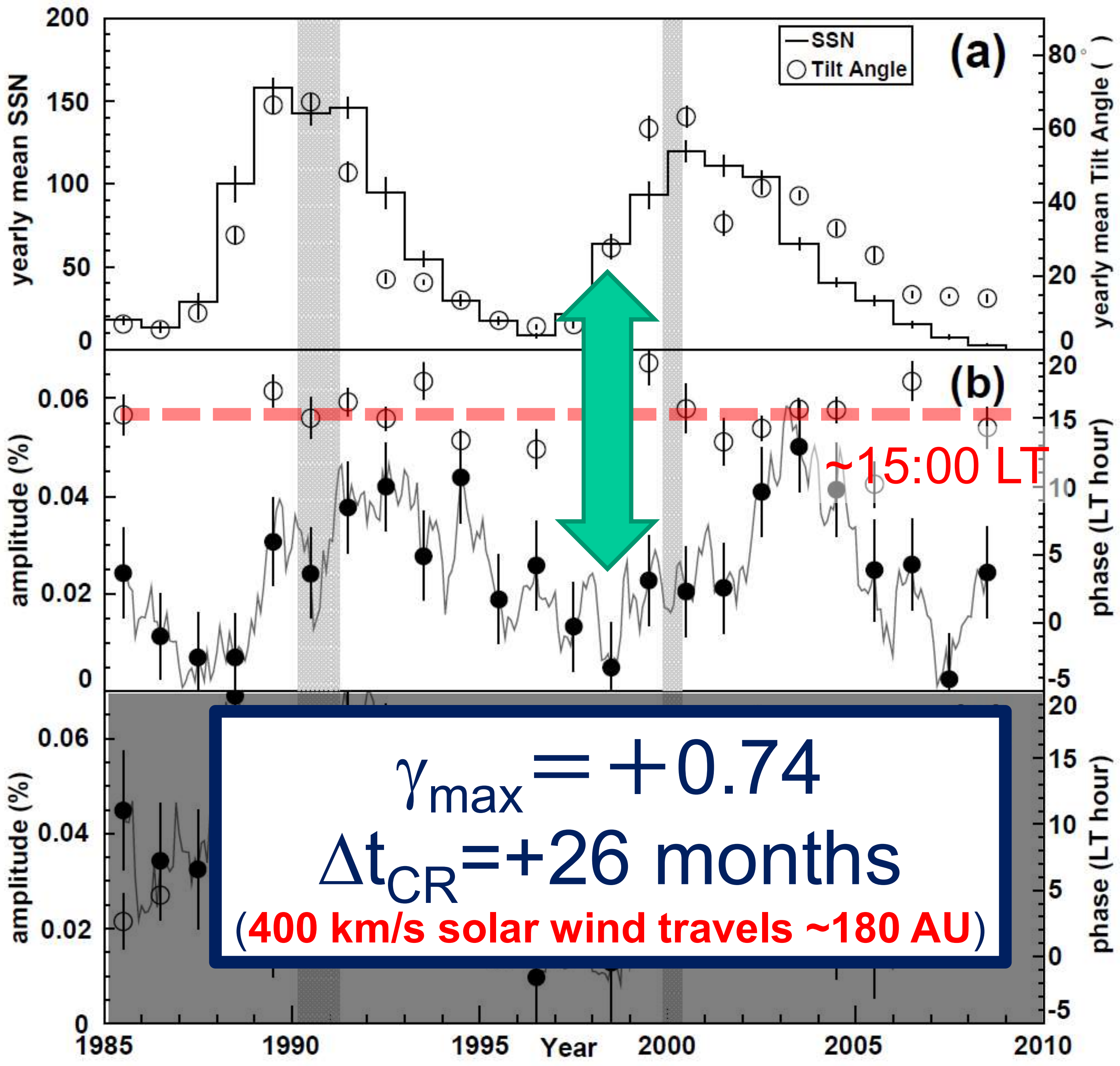

$\gamma_{max} = +0.74$

$\Delta t_{CR} = +26$ months

(400 km/s solar wind travels ~180 AU)

Solar activity

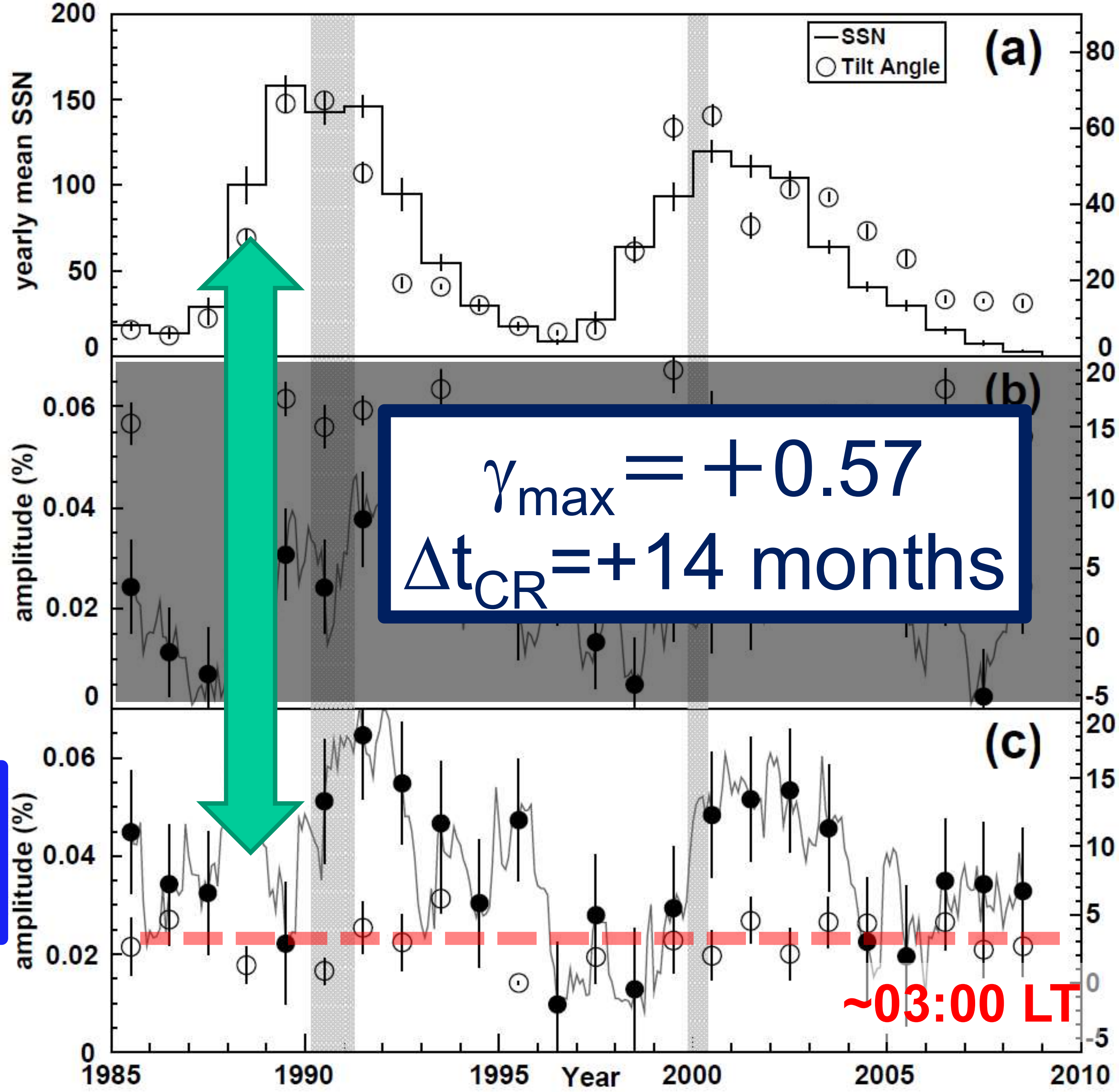

Solar
(CG-subtracted)

Sidereal

$\gamma_{max} = +0.57$

$\Delta t_{CR} = +14$ months

Steady increase of amplitude?

No significant correlation with the solar activity seen by Matsushiro

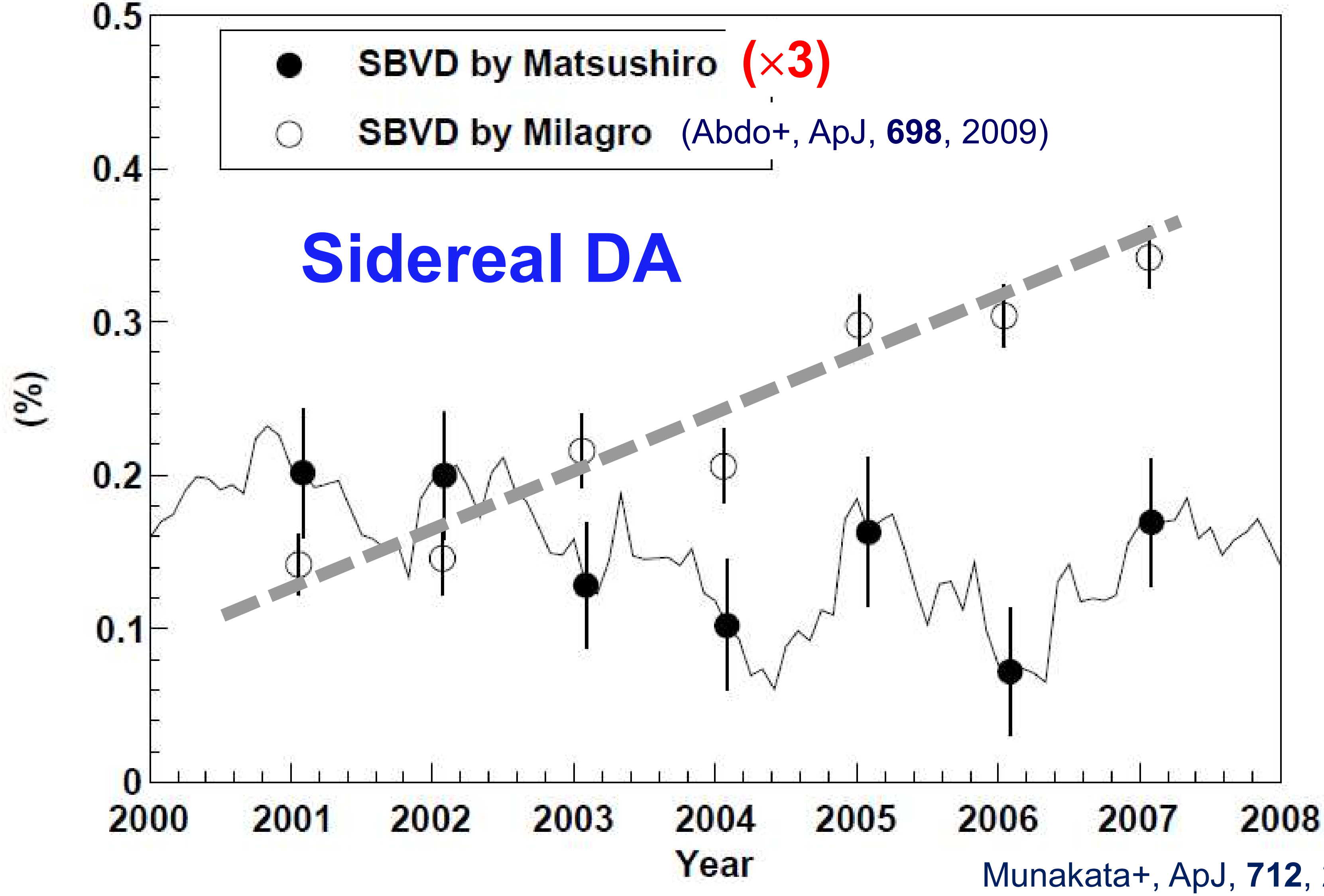

Munakata+, ApJ, **712**, 2010

Steady increase of amplitude?

No significant correlation with the solar activity confirmed by Tibet III

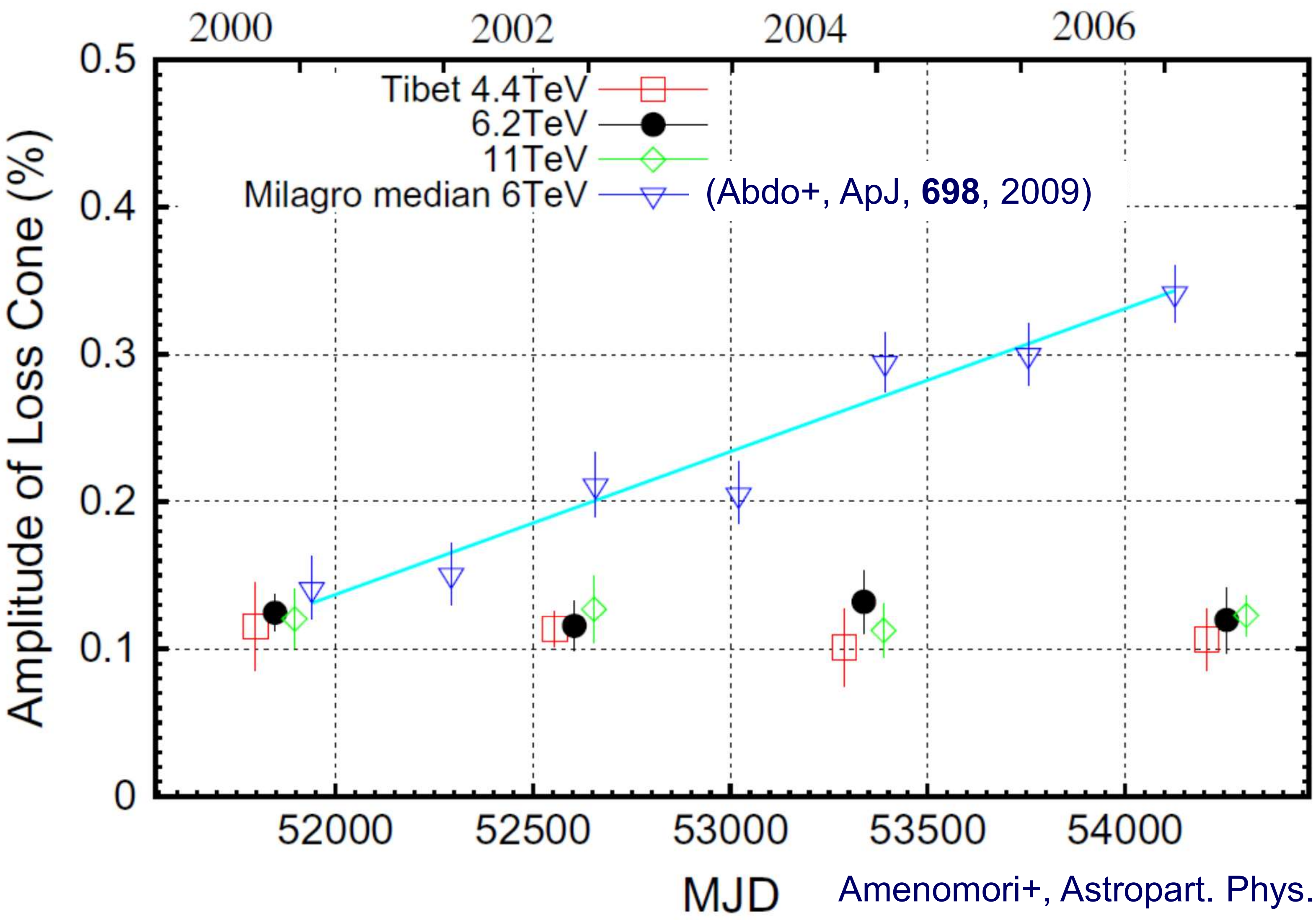

Amenomori+, Astropart. Phys., **36**, 2012

Small solar cycle variation

~1/6 (17%) variation only

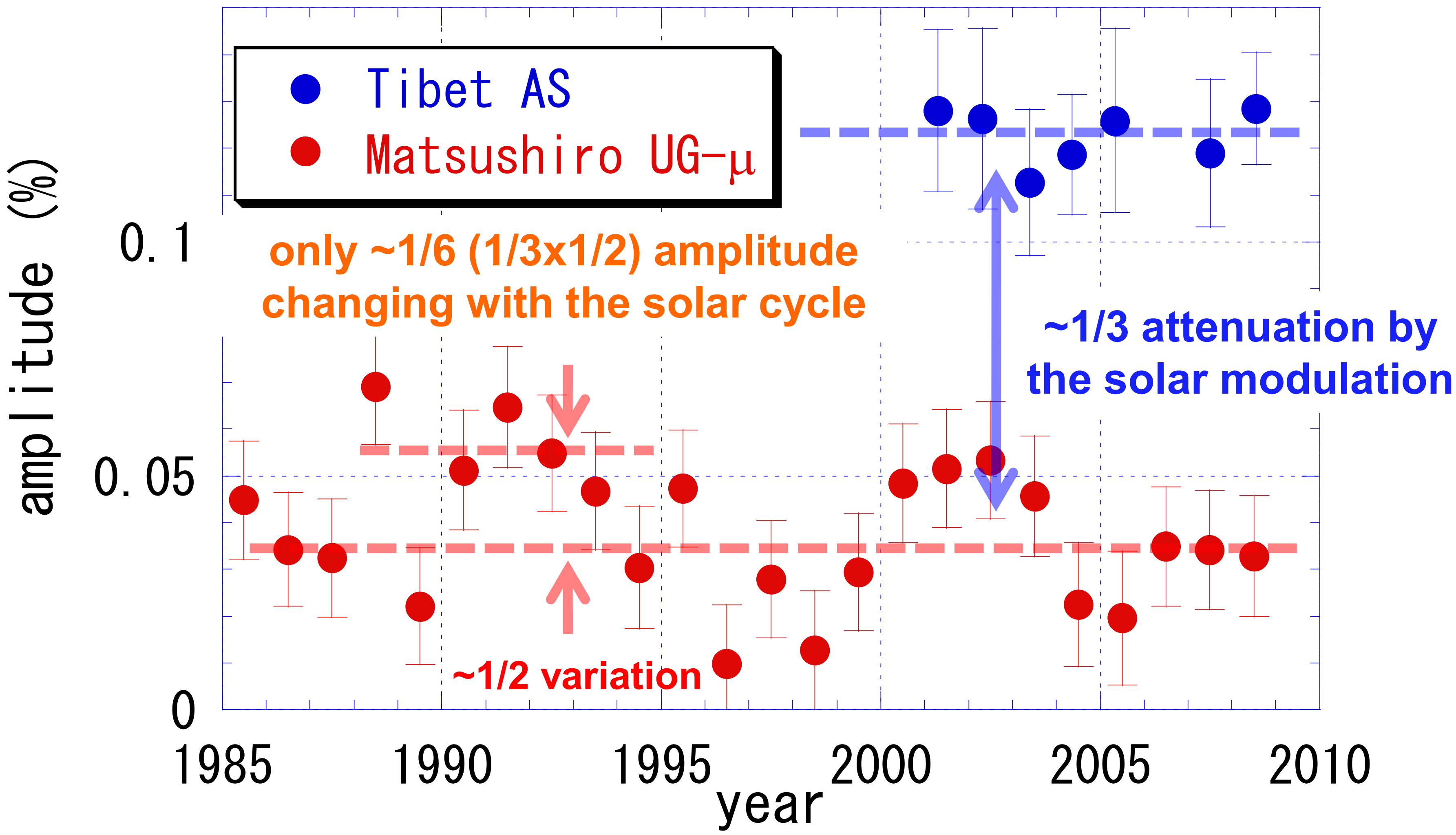

Prof. Y. Sekido

Mt. Norikura AS array

(Nagashima+, IL Nouvo Cim. **12C,** 1989)

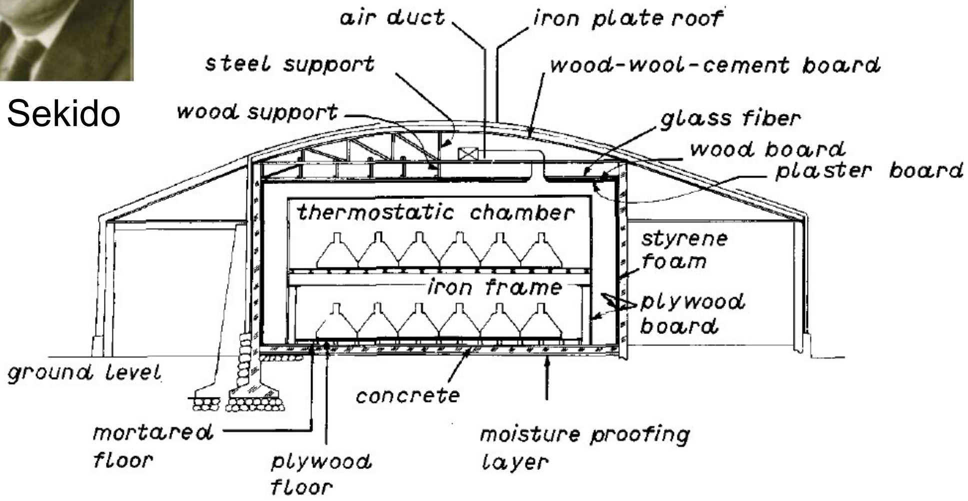

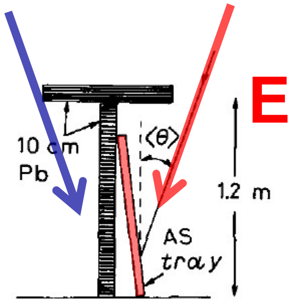

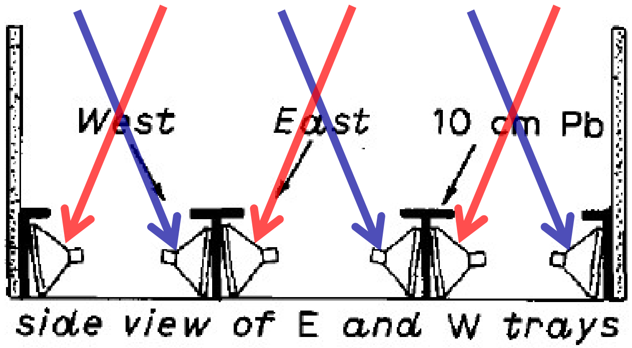

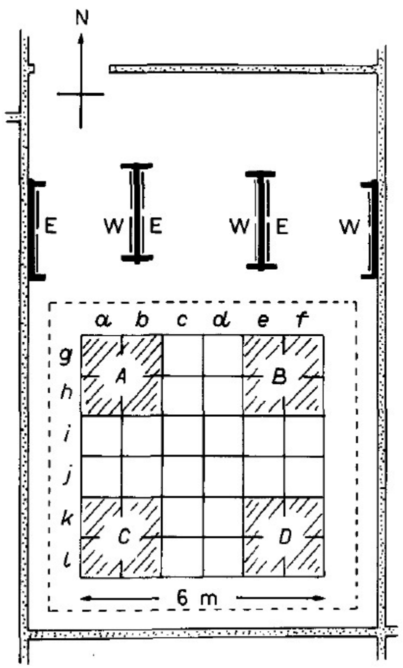

Operation started in 1973 @10 TeV

1D analyses of sidereal DA

Mt. Norikura AS-array (1973-1987)@10TV

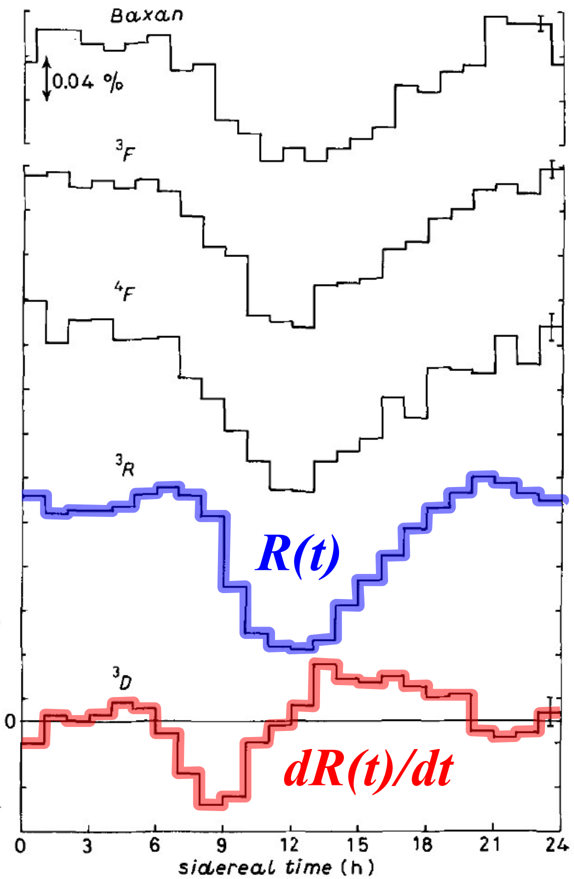

Tibet III-array (1999-2003)@10TV

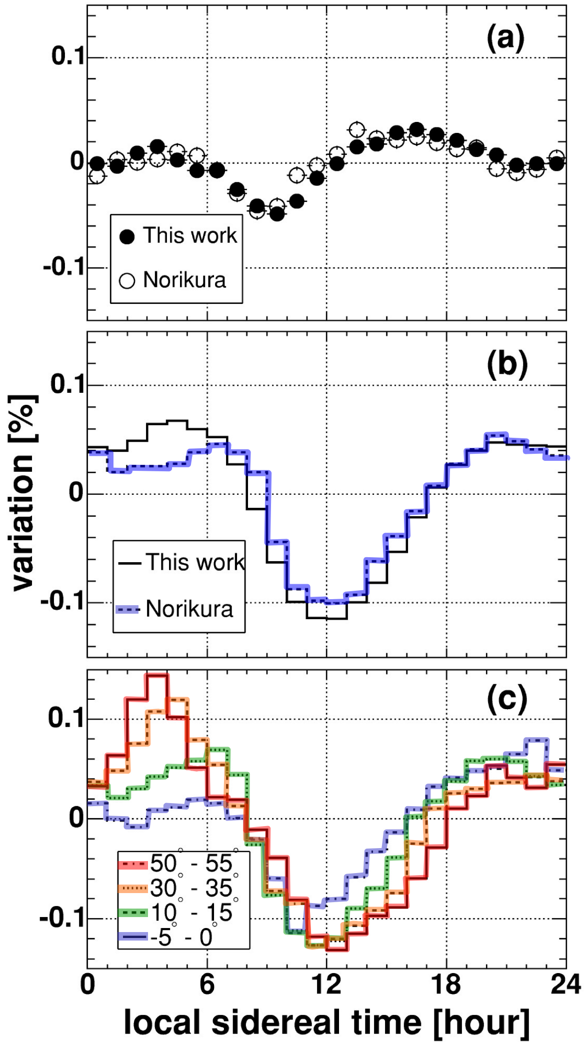

Amenomori+, ApJL, **626**, 2005

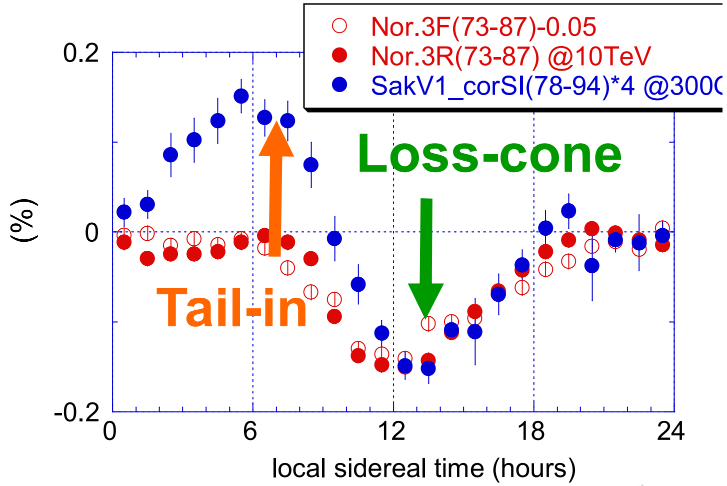

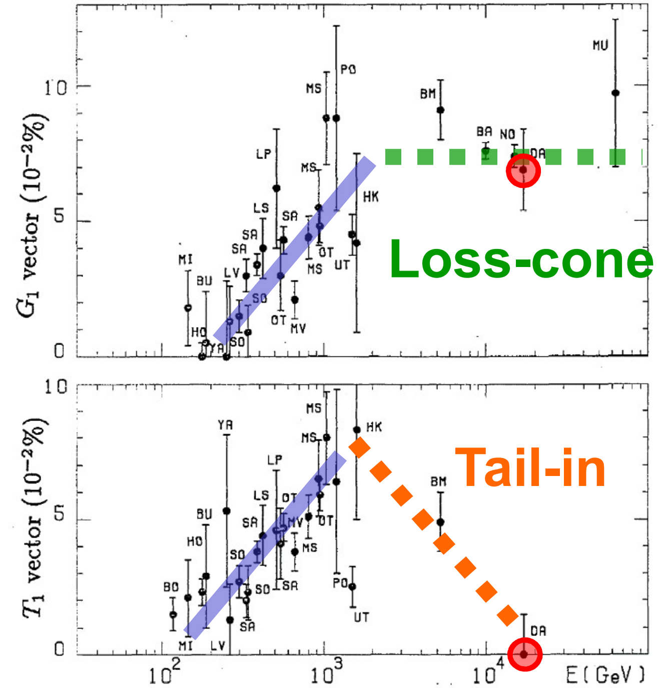

Nagashima+, JGR, **103**, 1998

Sidereal DA & semi-DA

Mt. Norikura (1973-87)

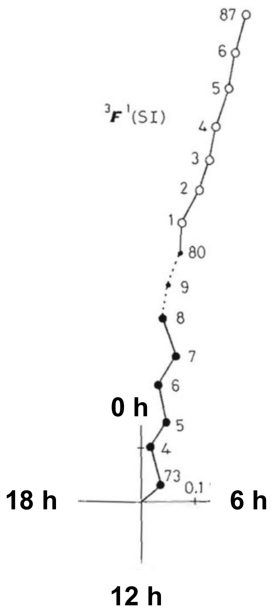

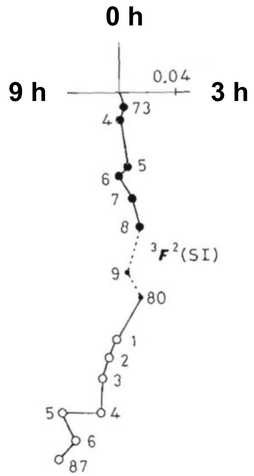

Tibet III (1999-2008)

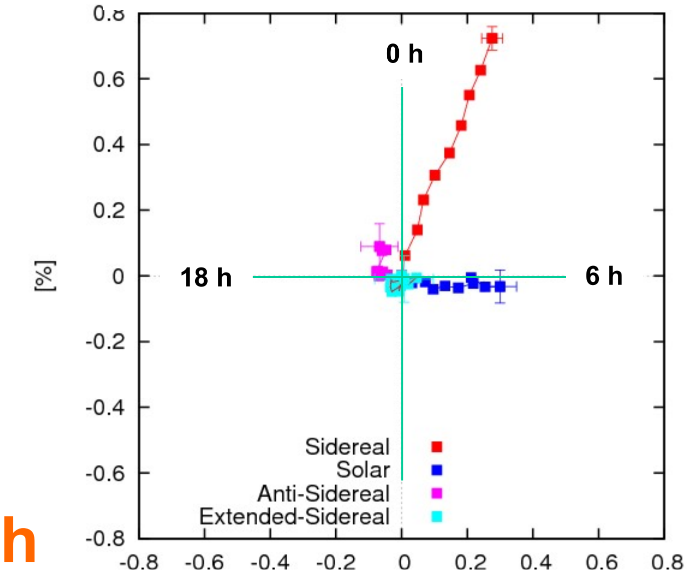

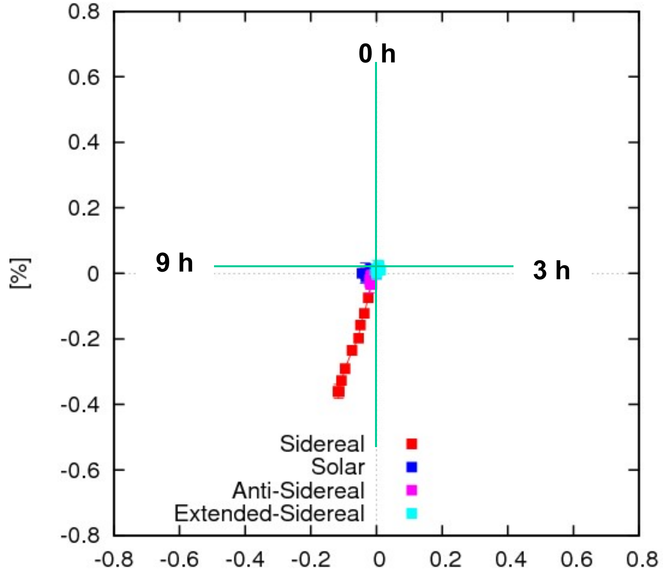

Sidereal DA

Max.@~0h
Min.@~12h

Narrow dip @~12h
⇒ "Loss-cone"

Sidereal semi-DA

Max.@~6h
Min.@~12h

Mid-scale Anisotropy model

(modeling Tail-in anisotropy)

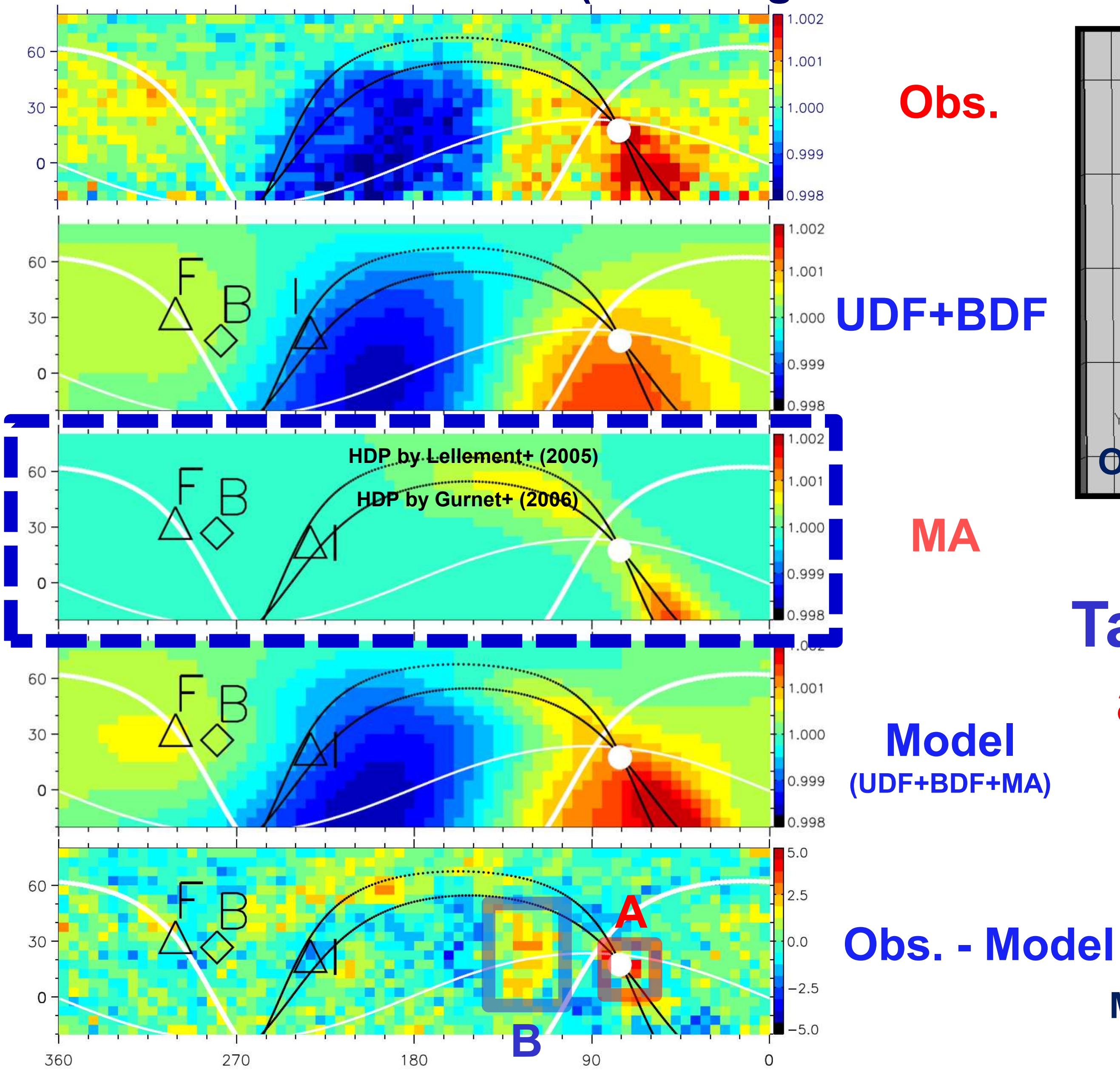

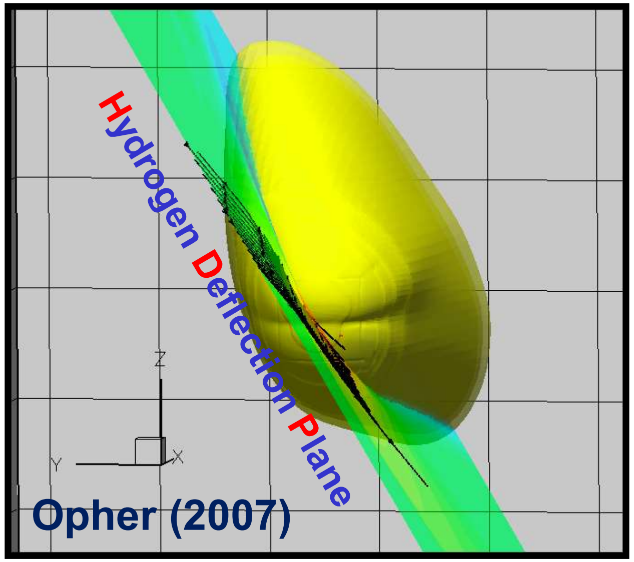

Tail-in anisotropy along the HDP

Miraglo "hot" regions A & B
(Abdo+, PRL, **101**, 2008)

Best-fit analysis of 2D map by Tibet III

Amenomori+, ASTRA, **6**, 2010

Original intensity | **Normalized in each dec.-band**

UDF

+

BDF

+

MA

=

Best-fit model

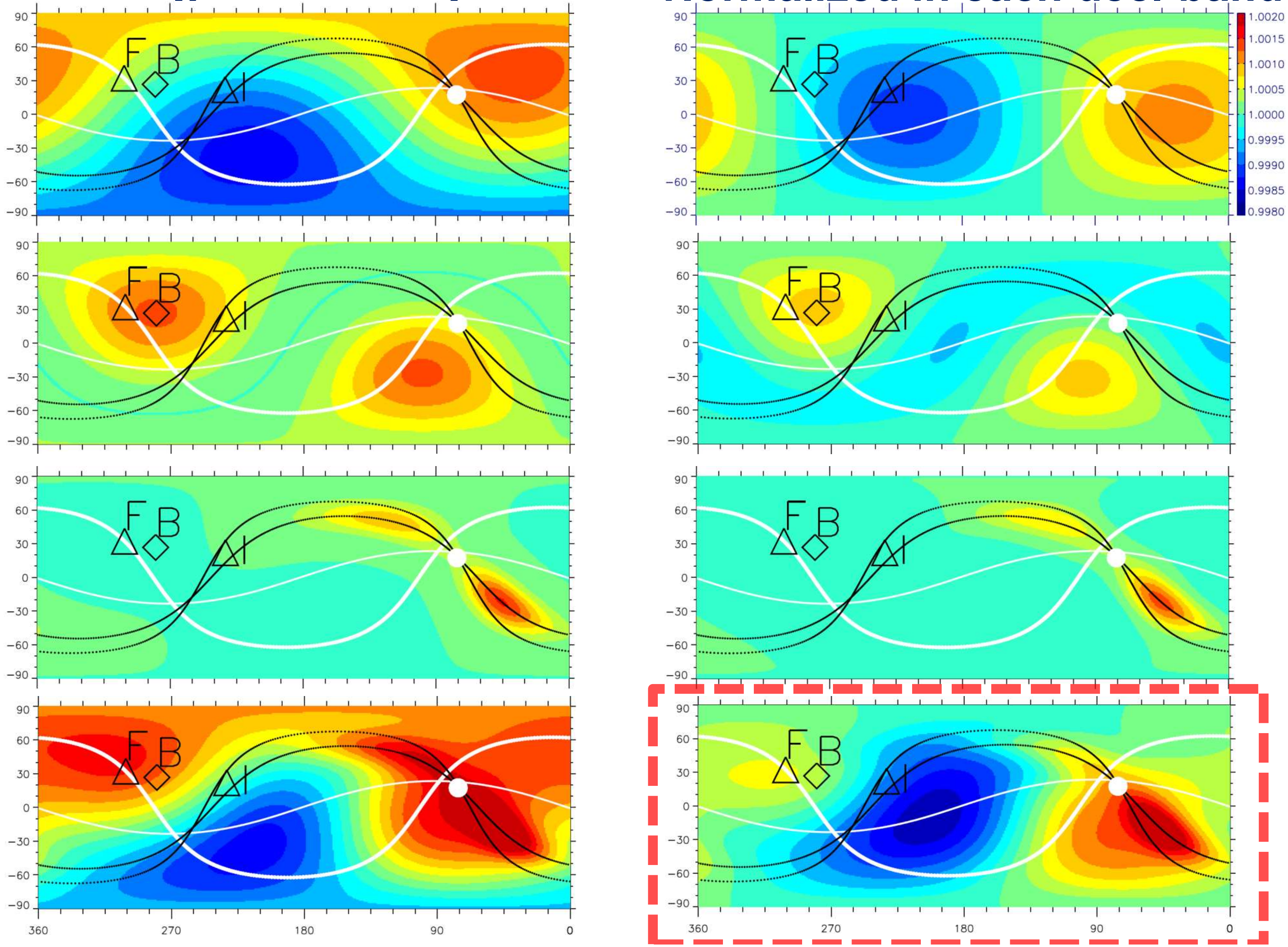

Local structure model (Mizoguchi+, proc. 31st ICRC, 2009)

Best-fit parameters (Amenomori+, ASTRA, **6**, 2010)

Uni-directional	Bi-directional
$a_{1\perp}$ =0.166%, $a_{1//}$ =0.038%	$a_{2//}$ =0.134%
$\alpha_{1\perp}$ =34.3°, $\delta_{1\perp}$ =39.3°	$\alpha_{2//}$ =99.3°, $\delta_{2//}$ =-27.7° (LIMF orientation)

For 5 TeV CRs…

Larmor radius : R_L~ 0.002 pc in 3μG field
Scattering m.f.p. : $\lambda_{//}$ ~ 3 pc
(e.g. Moskalenko et al., 2002)

$\xi_{//} \sim \lambda_{//}$ /L~0.001 ∴L ~ 3 kpc

Large-scale?

Bohm factor $\lambda_{//}/R_L$~ 1500 >> 1 (~10 in the heliosphere)

⇒ Perp. Diffusion flux is negligible

⇒ Only diamagnetic drift (ξ_T) can produce enough $\xi_\perp$

LIC and anisotropy

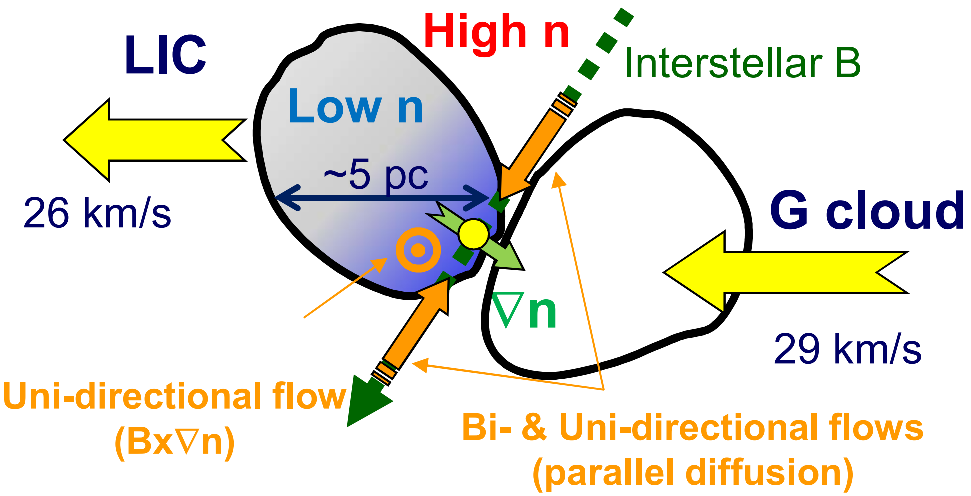

ξ_T~ R_L/L' ~0.001 ∴L' ~ 2 pc

Local-scale structure

is needed

Local structure model (Mizoguchi+, proc. 31st ICRC, 2009)

Best-fit parameters (Amenomori+, ASTRA, **6**, 2010)

Uni-directional	Bi-directional
$a_{1\perp}$ =0.166%, $a_{1//}$ =0.038%	$a_{2//}$ =0.134%
$\alpha_{1\perp}$ =34.3°, $\delta_{1\perp}$ =39.3°	$\alpha_{2//}$ =99.3°, $\delta_{2//}$ =-27.7° (LIMF orientation)

For 5 TeV CRs…

Larmor radius : R_L~ 0.002 pc in 3μG field
Scattering m.f.p. : $\lambda_{//}$ ~ 3 pc
(e.g. Moskalenko et al., 2002)

Billiard ball scattering model

$$\kappa_\perp/\kappa_\parallel = \frac{1}{1+(\lambda_\parallel/R_L)^2}$$

$$\kappa_T/\kappa_\parallel = \frac{\lambda_\parallel/R_L}{1+(\lambda_\parallel/R_L)^2}$$

Bohm factor $\lambda_{//}/R_L$~ 1500 >> 1 (~10 in the heliosphere)

⇒ Perp. Diffusion flux is negligible

⇒ Only diamagnetic drift (ξ_T) can produce enough $\xi_\perp$

LIC and anisotropy

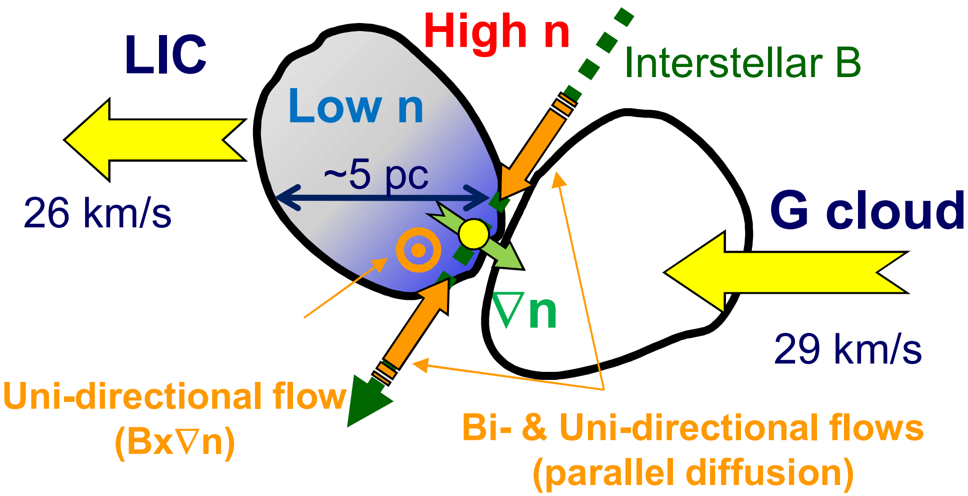

ξ_T~ R_L/L' ~0.001 ∴ L' ~ 2 pc

Local-scale structure
is needed

Local structure model (Mizoguchi+, proc. 31st ICRC, 2009)

Best-fit parameters (Amenomori+, ASTRA, **6**, 2010)

Uni-directional	Bi-directional
$a_{1\perp}$ =0.166%, $a_{1//}$ =0.038%	$a_{2//}$ =0.134%
$\alpha_{1\perp}$ =34.3°, $\delta_{1\perp}$ =39.3°	$\alpha_{2//}$ =99.3°, $\delta_{2//}$ =-27.7° (LIMF orientation)

For 5 TeV CRs…

Larmor radius : $R_L \sim$ 0.002 pc in 3μG field
Scattering m.f.p. : $\lambda_{//} \sim$ 3 pc
(e.g. Moskalenko et al., 2002)

Bohm factor $\lambda_{//} / R_L \sim$ 1500 >> 1 (~10 in the helio

⇒ **Per|**

⇒

LIC and anisotropy

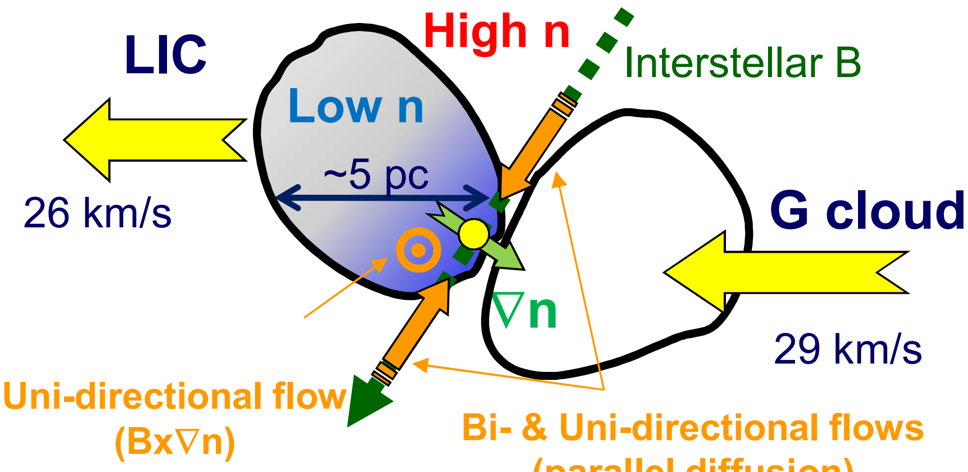

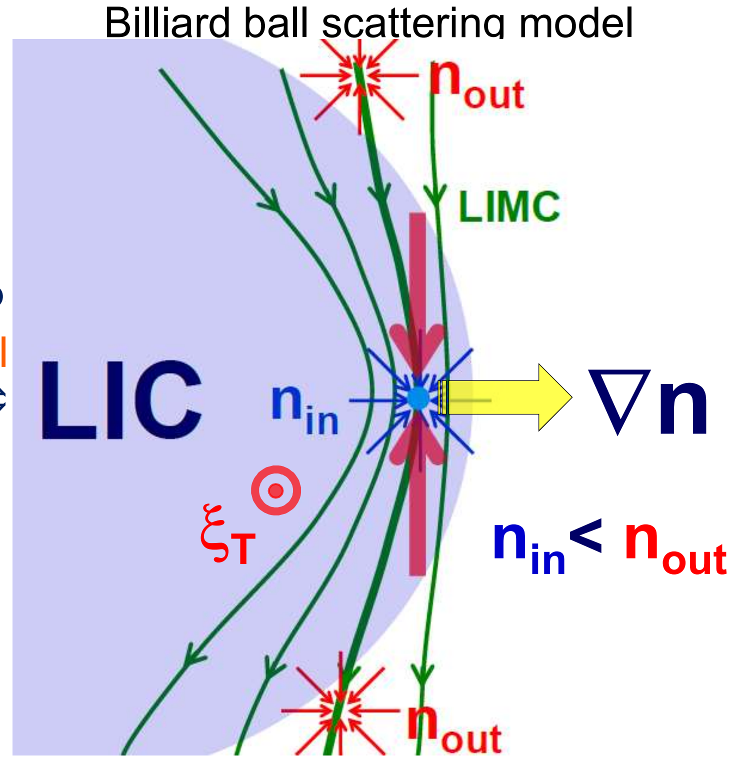

Local-scale structure
is needed

CR modulation in a MHD heliosphere

(Zhang+, ApJ, **790**, 2014)

- **Apply Liouiville's theorem.**
- **Back-trace of CR-orbit from Earth to boundary set at 1000 AU.**
- **Obtain UDF & BDF outside boundary, best reproducing Tibet's model 2D map.**
- **No interpretation for the UDF & BDF.**

- **Tail-in anisotropy along HDP is reproduced.**
- **Significant modulations of UDF & BDF are suggested.**

Tibet's model 2D map

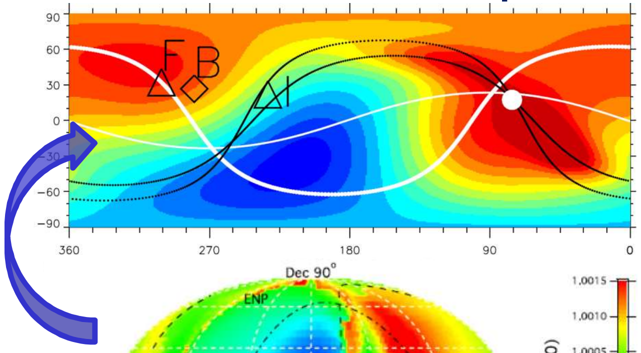

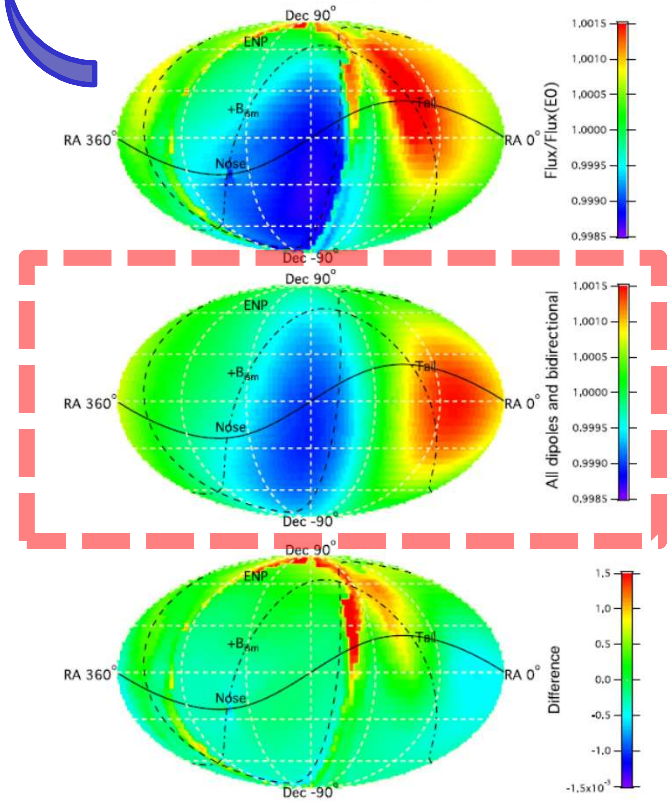

Figure 9. Top: map of composite anisotropy from Equation (14) with best fit parameters in Table 1, (middle) map of a superposition of dipoles and bidirectional anisotropies in the LISM without heliospheric influence, and (bottom) the difference between the top and middle maps.

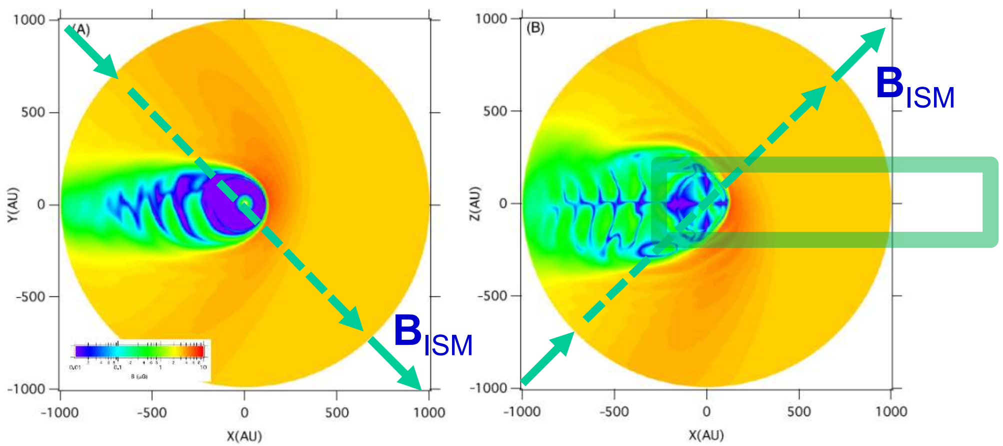

Time-dependent MHD heliosphere

(with 11y & 22y variations)

CR modulation in a MHD heliosphere

(Zhang+, ApJ, **790**, 2014)

- **Apply Liouiville's theorem.**
- **Back-trace of CR-orbit from Earth to boundary set at 1000 AU.**
- **Obtain UDF & BDF outside boundary, best reproducing Tibet's model 2D map.**
- **No interpretation for the UDF & BDF.**

- **Tail-in anisotropy along HDP is reproduced.**
- **Significant modulations of UDF & BDF are suggested.**

Tibet's model 2D map

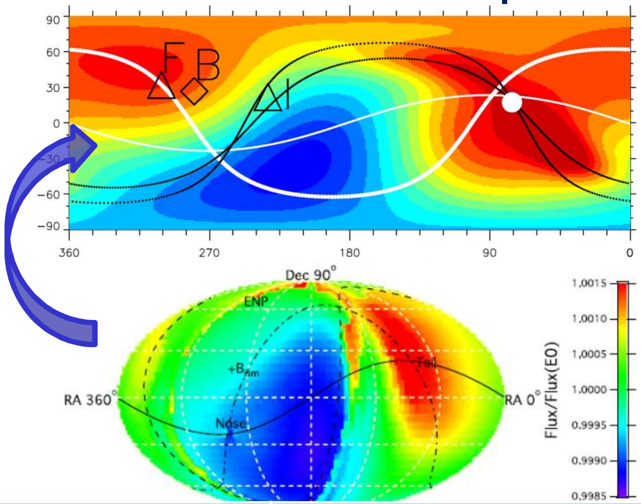

	$a_{2\parallel}$ (%)		$a_{1\parallel}$ (%)		$a_{1\perp}$ (%)		$R_L G_\perp$ (%)	
	α (°)	δ (°)	—	—	α (°)	δ (°)	α (°)	δ (°)
Amenomori+ (2010)	0.134		0.038		0.166		0.166	
	99.3	-27.7	—	—	34.3	39.3	344	-52.3
Zhang+ (2014)	0.051		0.121		0.071		0.071	
	245	9	—	—	343	43	144	46

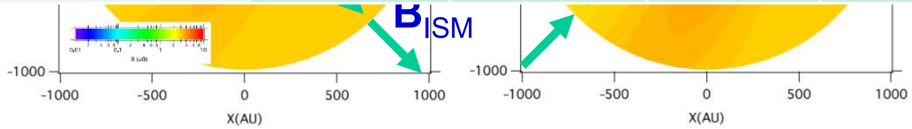

Time-dependent MHD heliosphere
(with 11y & 22y variations)

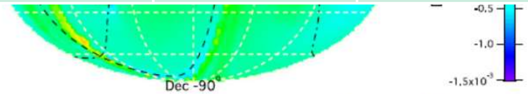

Figure 9. Top: map of composite anisotropy from Equation (14) with best fit parameters in Table 1, (middle) map of a superposition of dipoles and bidirectional anisotropies in the LISM without heliospheric influence, and (bottom) the difference between the top and middle maps.

Summary

- Amplitude of the Sidereal DA (SDA) below 1 TeV increases with energy (heliosphere becomes transparent due to the reduction of the solar modulation).
- SDA in about 0.5~50 TeV has eigen phases at 6 hr (Tail-in) and 0 hr (Loss-cone).
- Tail-in anisotropy is observed along the Hydrogen Deflection Plane (HDP).
- The SDA in about 1~50 TeV might be considerably reorganized (deformed) when observed at Earth through the heliosphere.
- The SDA shows new features above 100 TeV.

Cosmic ray shadow of the Sun
(Sun shadow)
observed by Tibet III

Sun Shadow

Sun Shadow

Sun blocks VHE cosmic rays, and cast the cosmic-ray shadow on the earth.

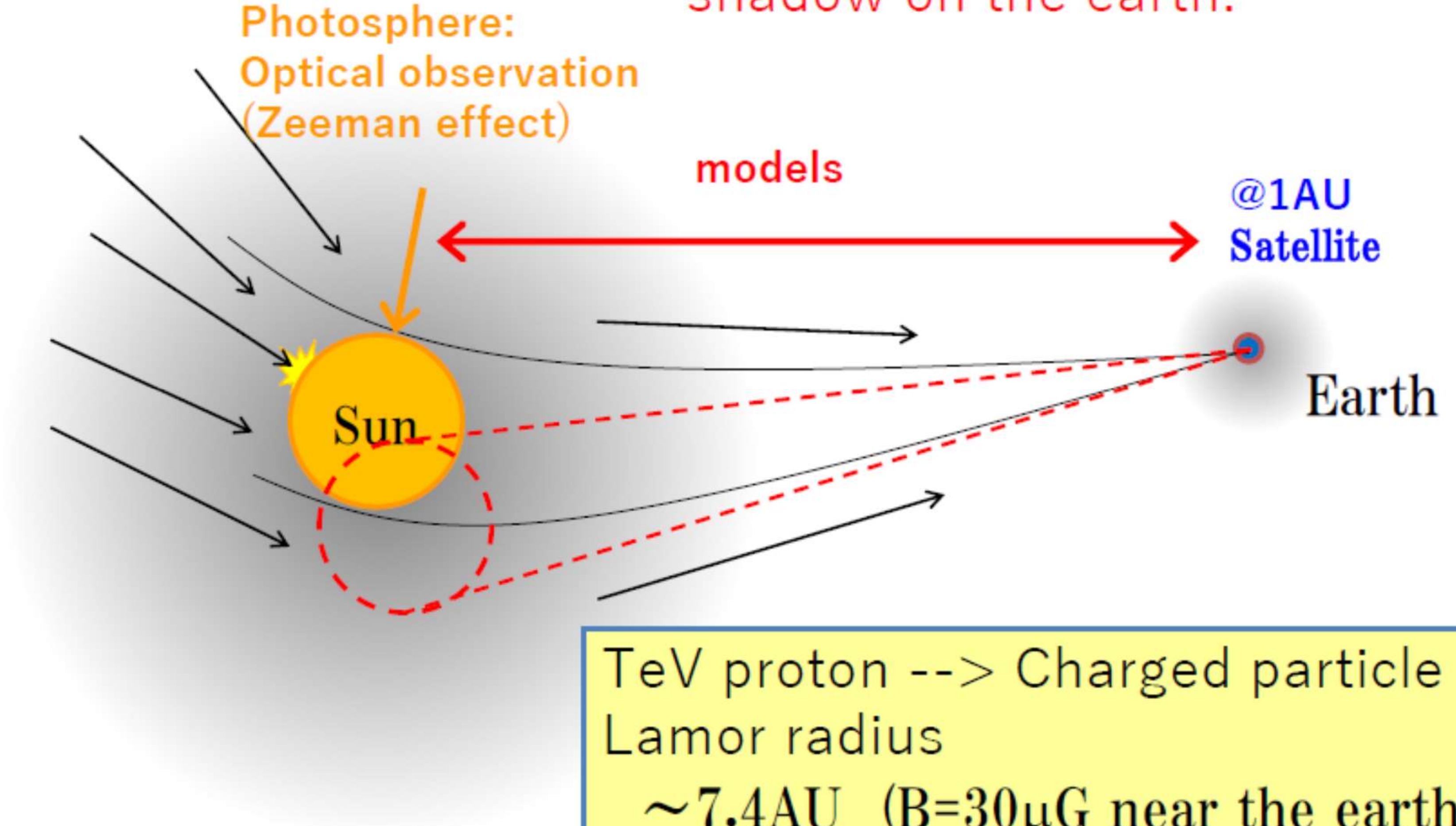

TeV proton --> Charged particle
Lamor radius

$\sim$7.4AU (B=30μG near the earth)

$\sim 0.16R_\odot$(B=300mG near the sun)

→ Probe of the solar MFs !

Past Results (Tibet-II >10TeV)

Amenomori et al, PRL, 111, 011101 (2013)

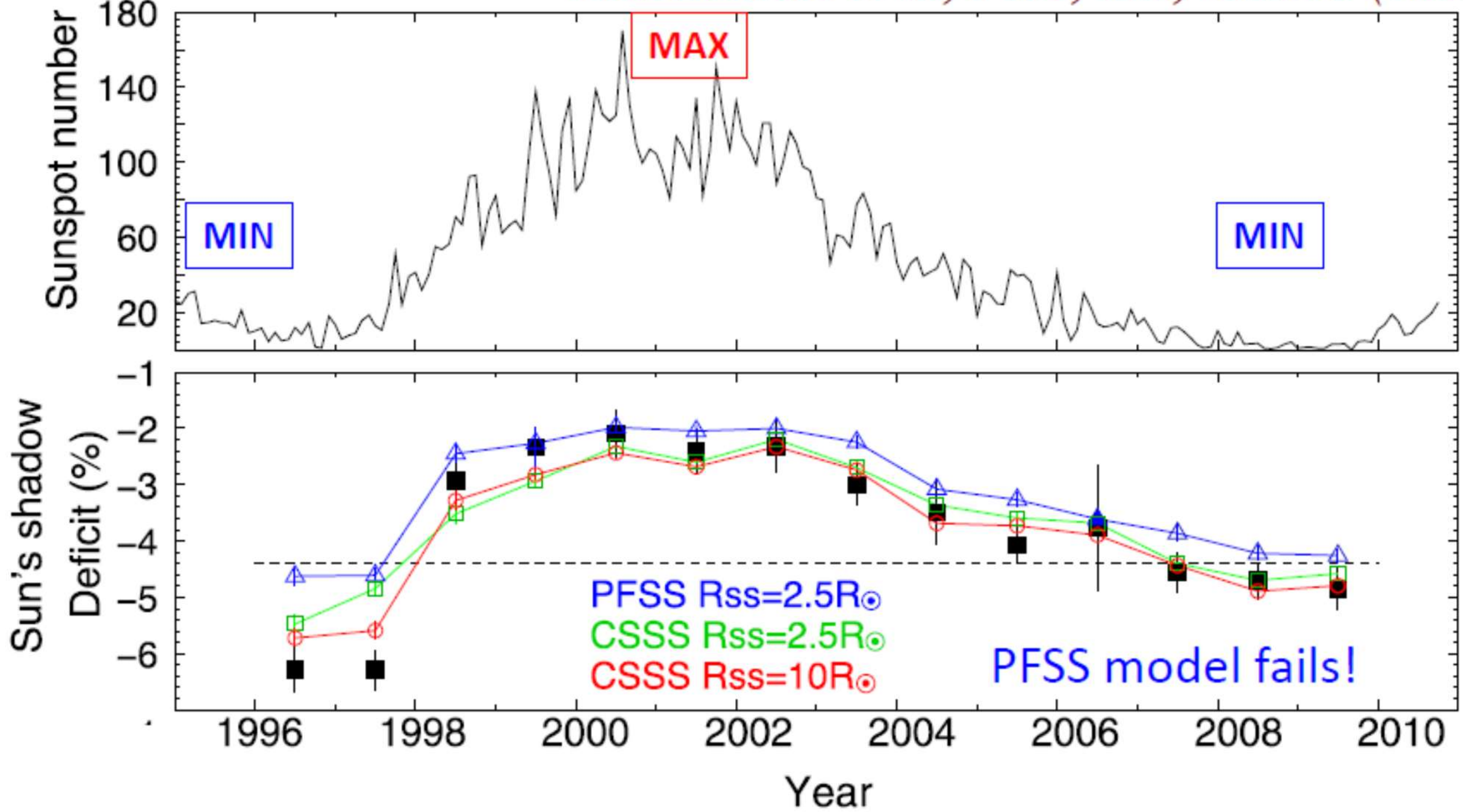

- ✓ Discovery of a clear anti-correlation of the deficits with SN
- ✓ Comparison b/w coronal MF models (PFSS/CSSS)

Sun Shadow Observation@3TeV

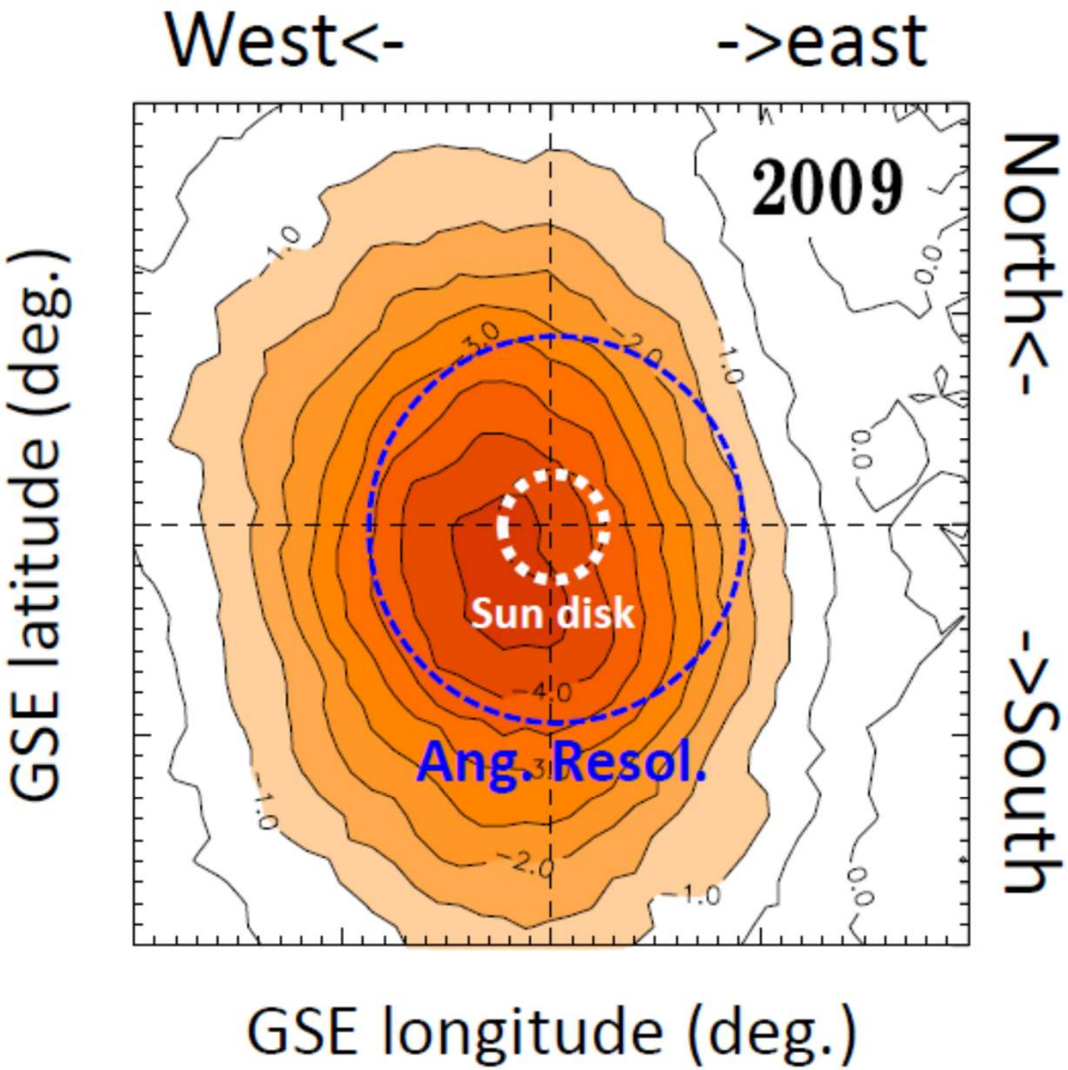

4°x 4° Cosmic ray density map centered at the Sun (GSE coordinate)

Deficit ratio to B.G.
Maximum -4%.

Optical disk size(0.26°)
Angular resolution(0.9°)

In this map, we analyze deficit and location varying in correlation with the solar magnetic field

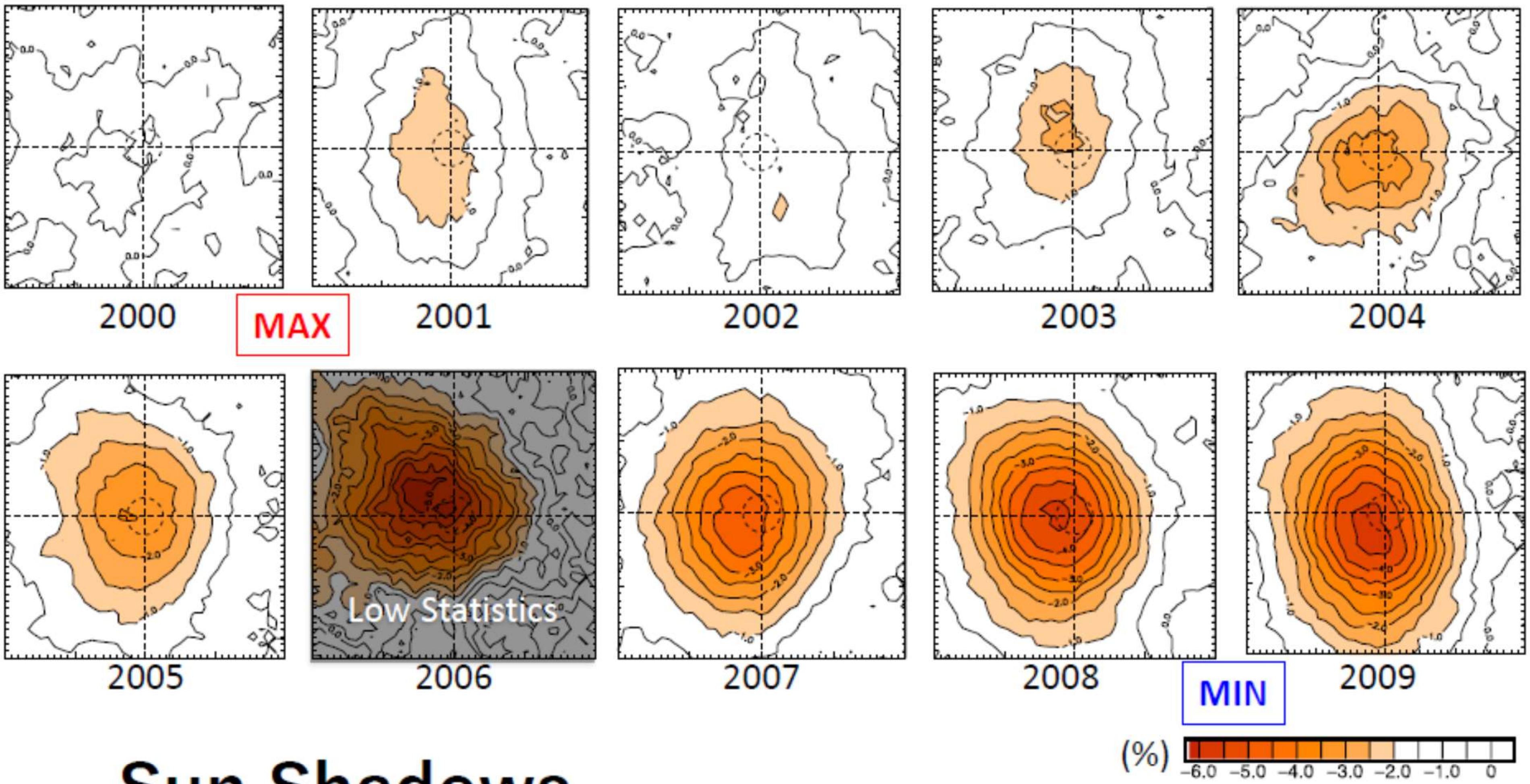

Sun Shadows
Tibet-III 3TeV
Deficit/B.G.(%)

Similar features at
10 TeV observation

Deficit – Obs/MC **All Data** - 3 TeV

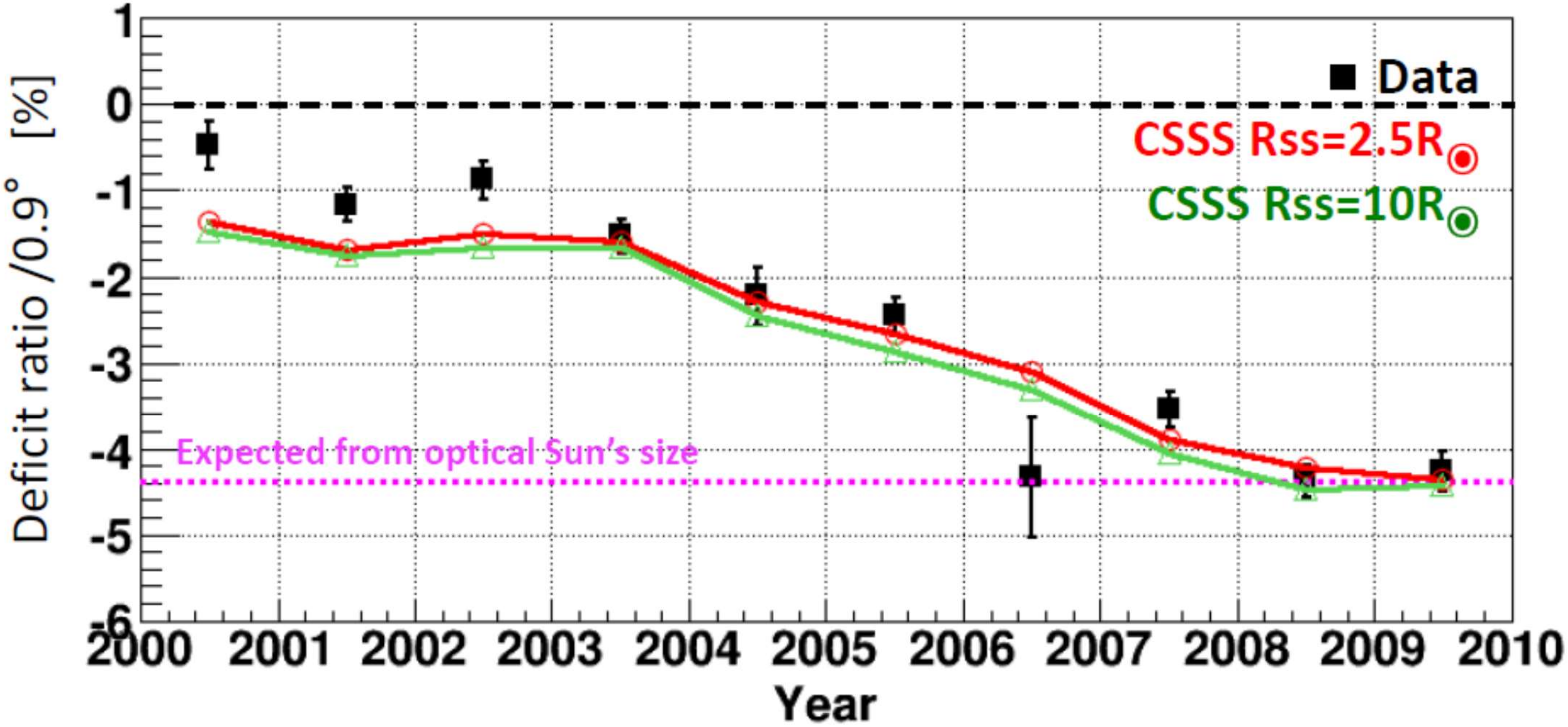

χ^2 test :

χ^2 / dof = 32.1 / 10 (3.4σ)

χ^2 / dof = 46.9 / 10 (4.8σ)

*only stat. error

CSSS does not reproduce well at the solar maximum

Influence of CMEs?

http://www.srl.caltech.edu/ACE/ASC/DATA/level3/icmetable2.htm

ICME Catalog

Richardson & Cane, Solar Phys (2010)

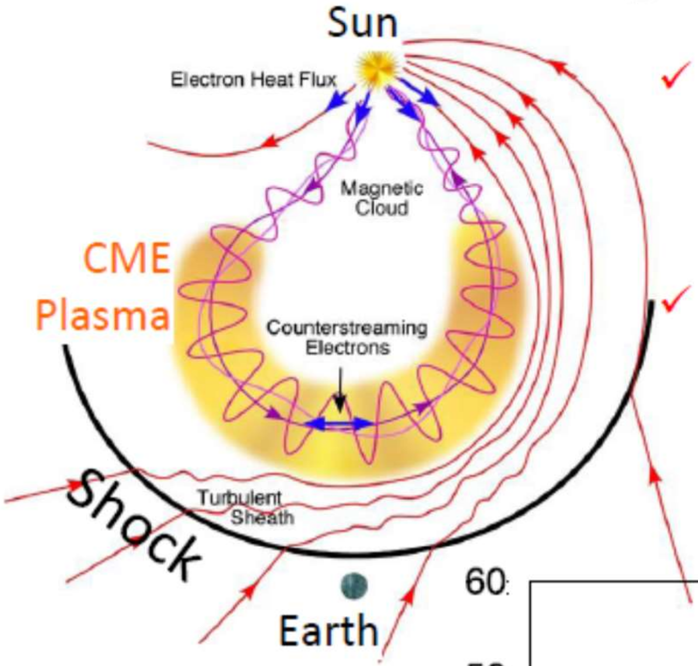

✓ Interplanetary Coronal Mass Ejection (ICME)
- CMEs interact with the solar wind and the IMF.
  - ICMEs in the near-Earth solar wind are listed.

✓ Exclude transit periods of ICMEs from the analysis
- ICME start is the eruption time at the Sun
- ICME end is plasma end at the earth.
- ICME transit period is ~4 ± 1 days

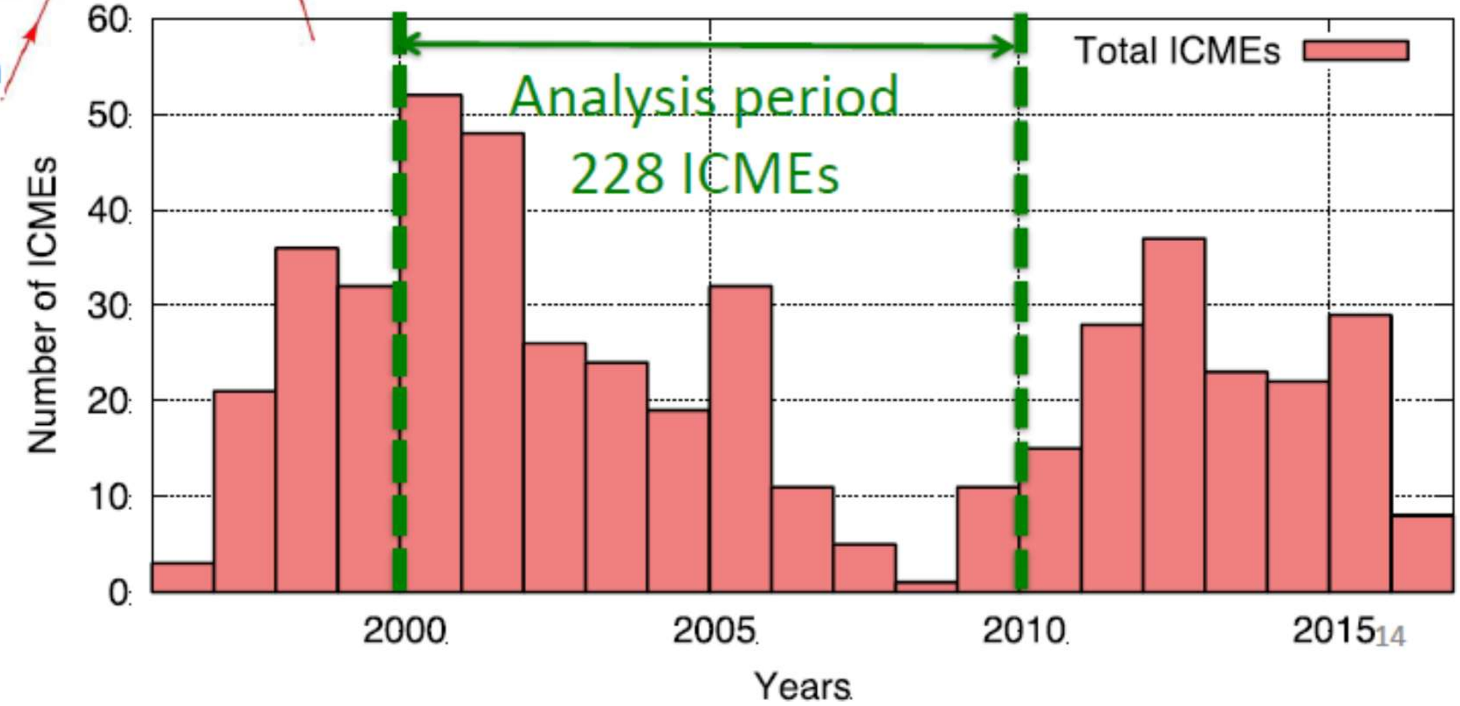

Deficit – Obs/MC **Excluding ICMEs** - 3 TeV

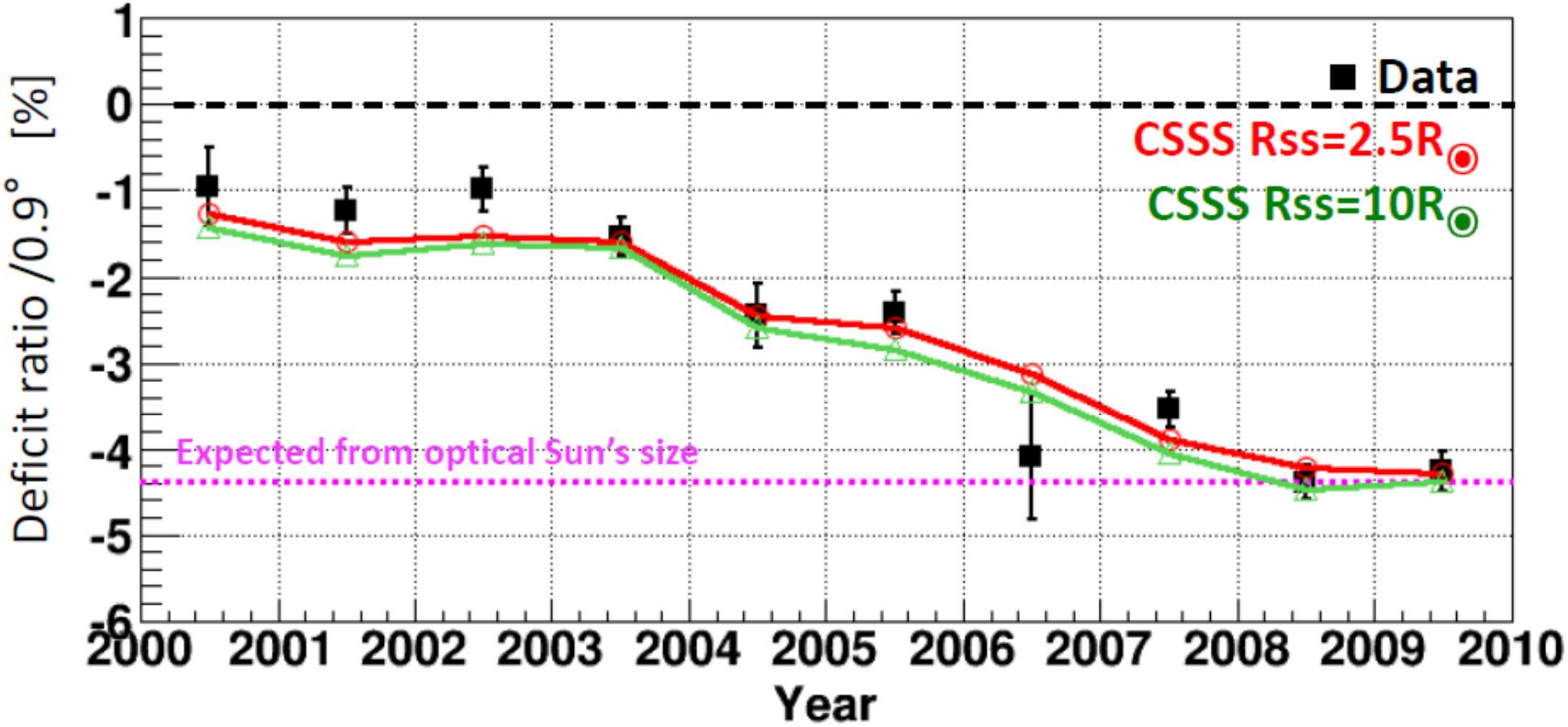

χ^2 test :

χ^2 / dof = 12.2 / 10 (0.6σ)

χ^2 / dof = 21.0 / 10 (2.0σ)

*only stat. error

Excluding ICMEs → CSSS works
Evidence for influence of ICMEs on the Sun shadow at 3 TeV

Deficit – Obs/MC **All Data** - 3 TeV

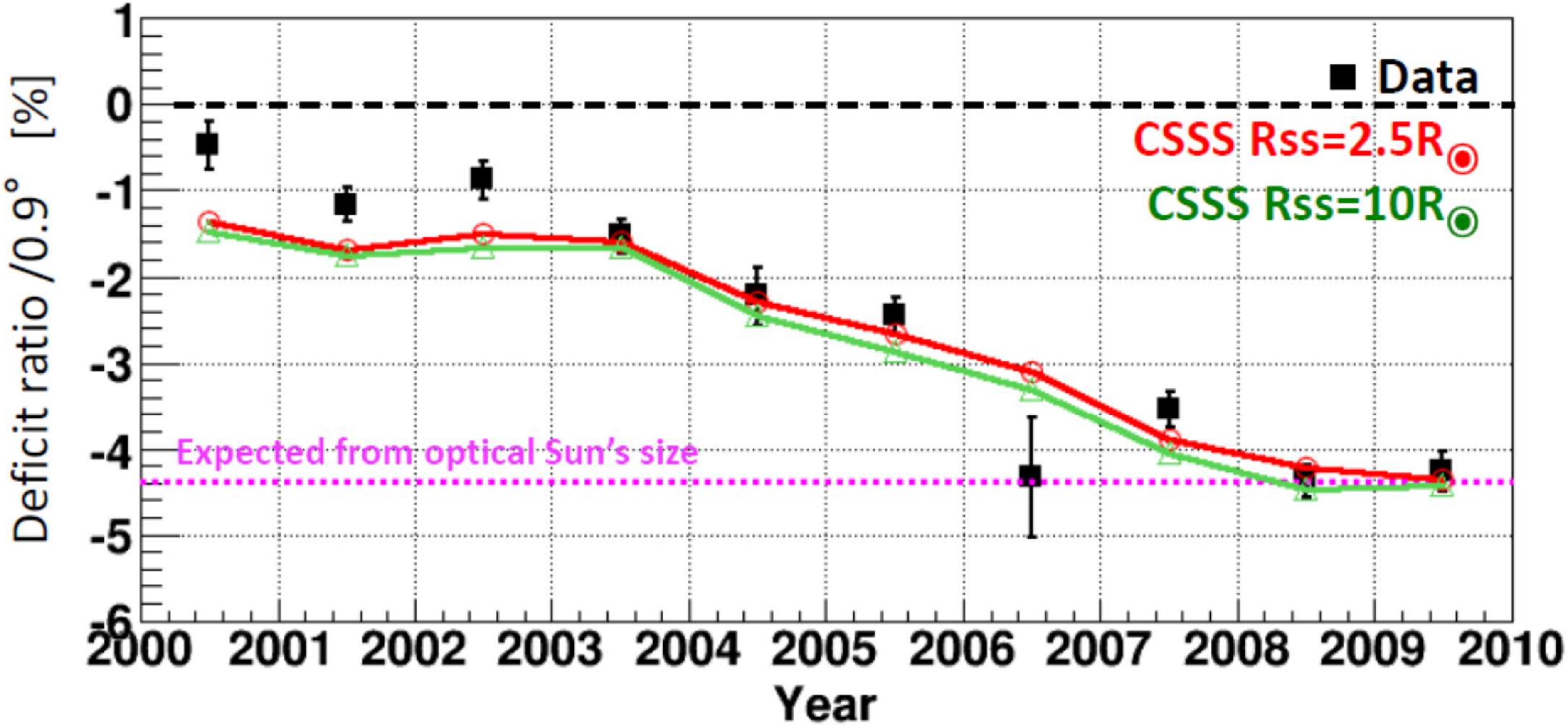

χ^2 test :

χ^2 / dof = 32.1 / 10 (3.4σ)

χ^2 / dof = 46.9 / 10 (4.8σ)

*only stat. error

CSSS does not reproduce well at the solar maximum

Influence of CMEs?

Sun's Shadow and IMF Sector Polarity

- The Sun's shadow is deflected northward (southward) in Away (Toward) sector by B_y

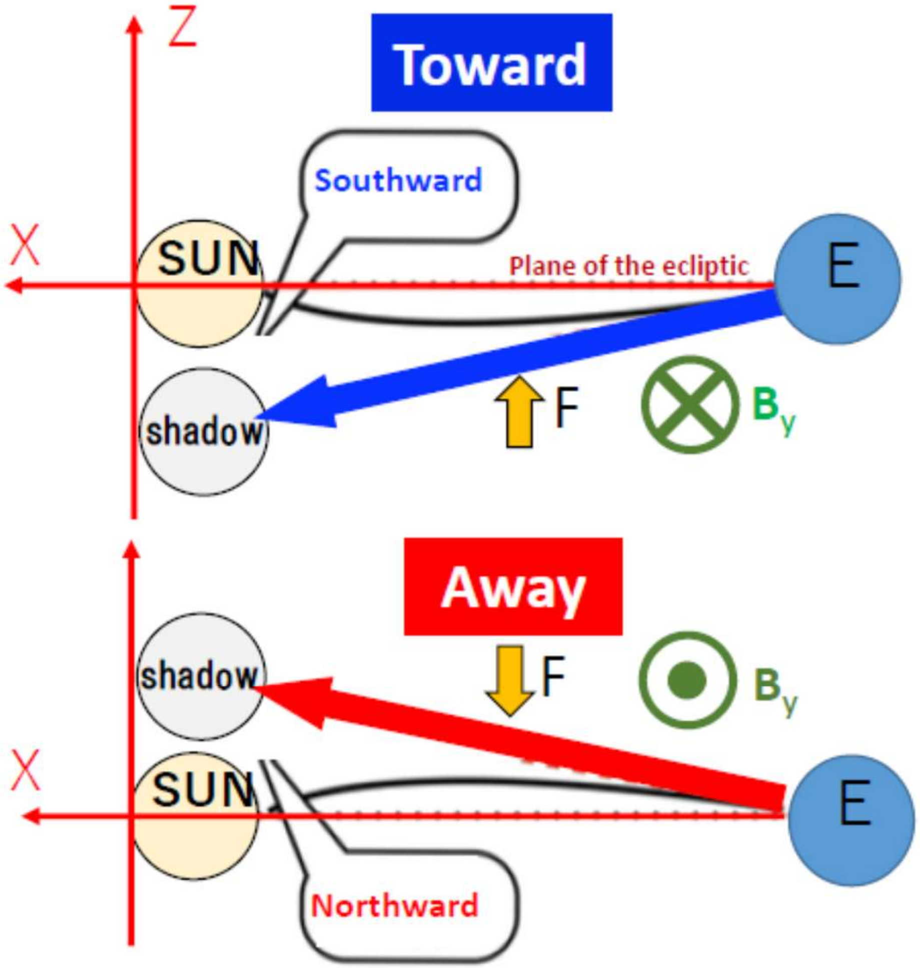

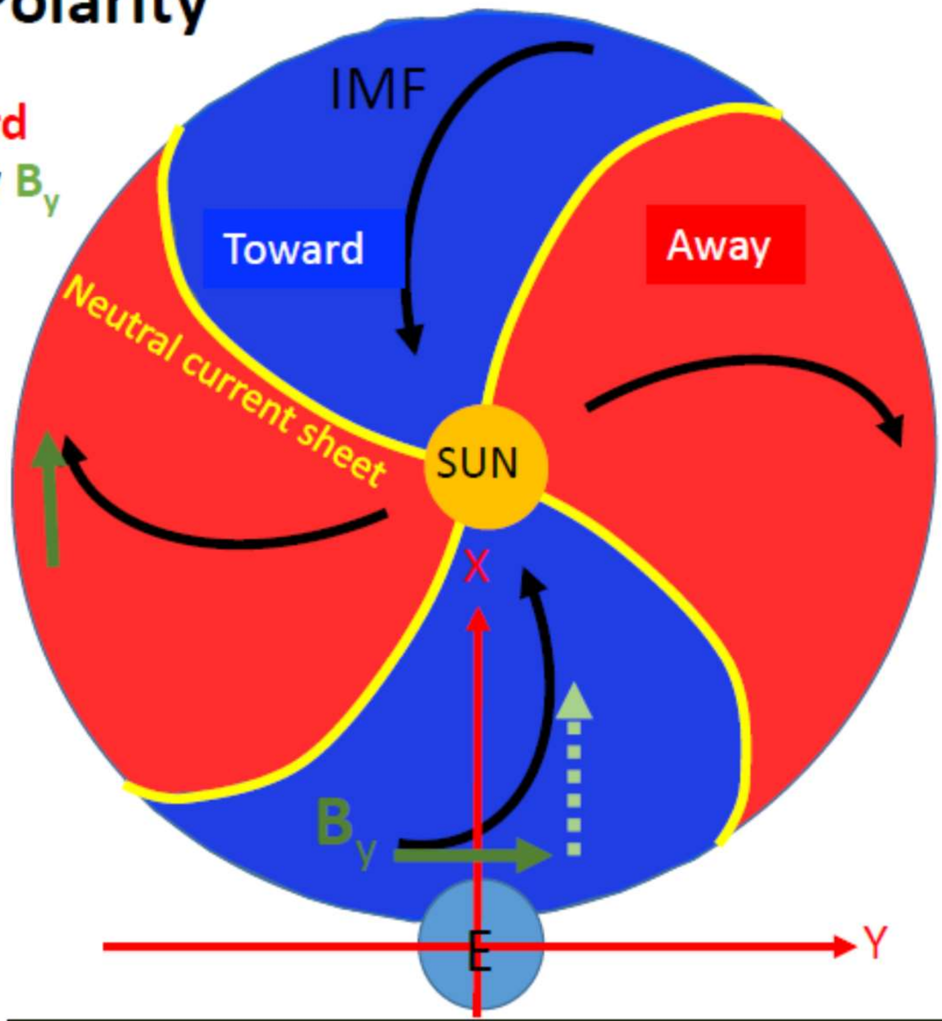

Assignment of the sector polarity with B_x & B_y observed two days later

$B_x < 0$ & $B_y > 0$ => Away

$B_x > 0$ & $B_y < 0$ => Toward

Observed Sun's shadow @13TV

- The center of Sun's shadow clearly deviates from the center of the Sun.
- North-South(N-S) displacement in Away(Toward) sector is Northward (Southward).

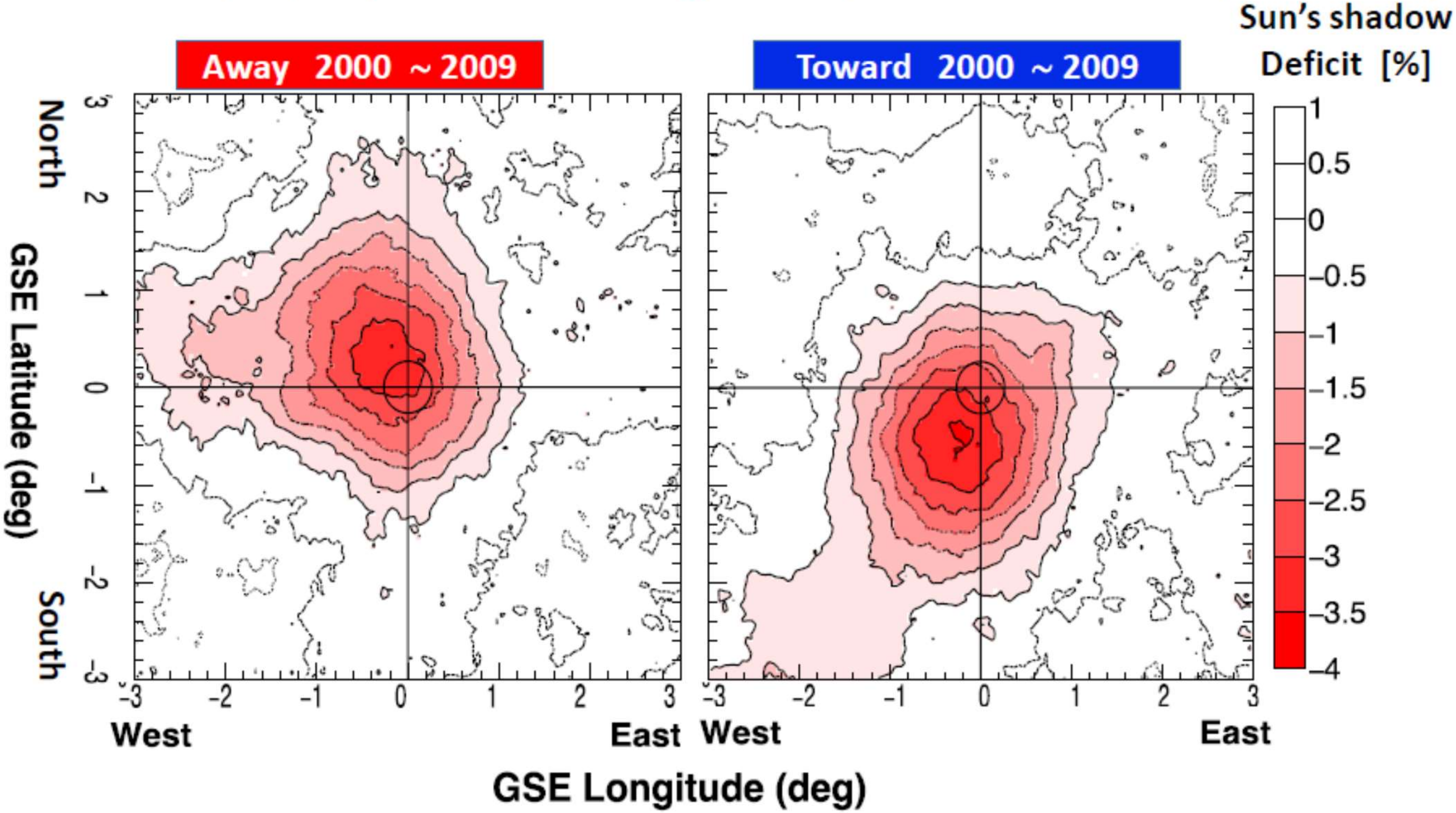

・Westward displacement is mainly due to the deflection in the geomagnetic field, as observed in the Moon's shadow.

Tibet-III : North – South Displacement of the Sun's Shadow

- **Rigidity (E/Ze) Dependence of N-S displacement, fitted by $f(R) = \alpha/(R/10[TV])$, fitting parameter: α denoting displacement angle at 10TV**
- **Our MC simulation underestimates α in both sectors!**

⇒the solar magnetic field model underestimates IMF strength between Sun and Earth!?

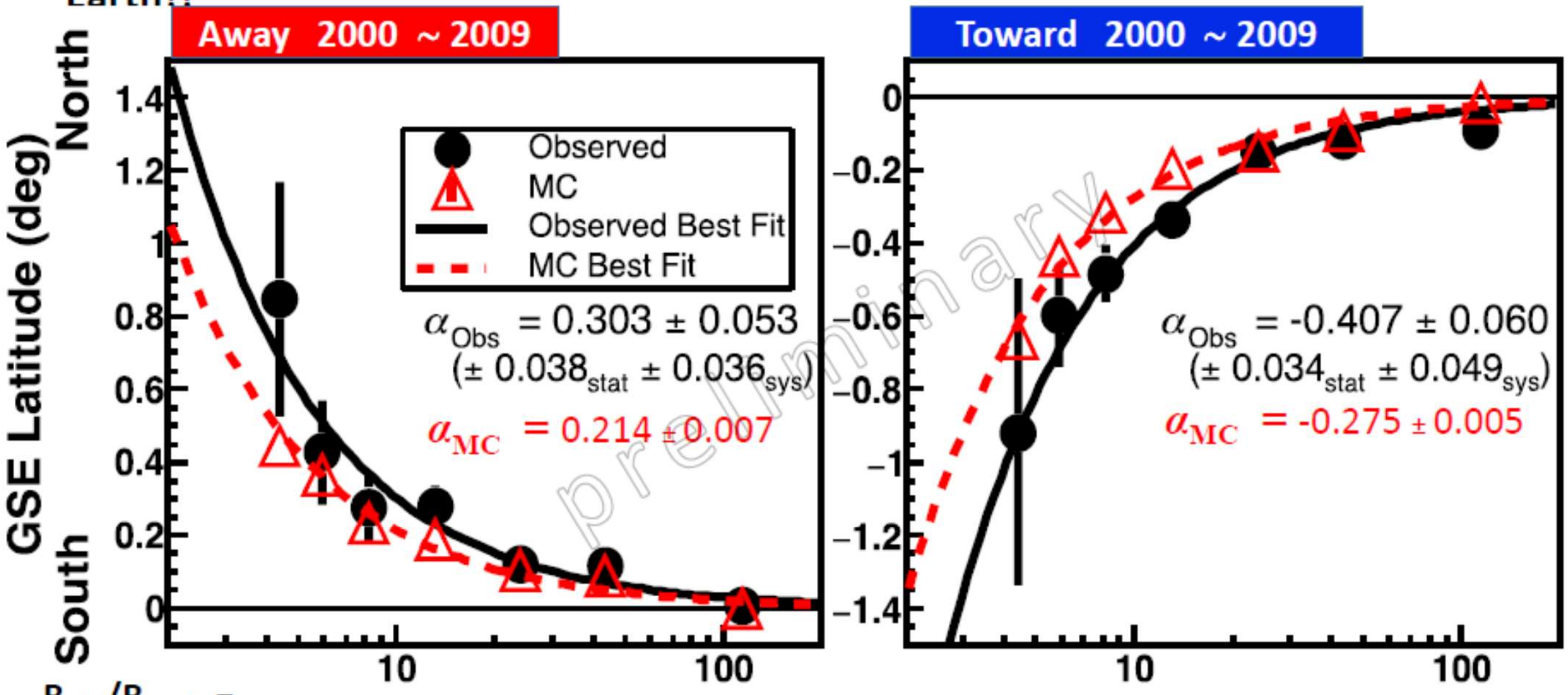

B_{obs}/B_{model}=

($1.54 \pm 0.21_{stat} \pm 0.20_{sys}$) (Away)

($1.62 \pm 0.15_{stat} \pm 0.22_{sys}$) (Toward)

Comparison b/w the observed (OMNI) & simulated IMF strengths@1AU

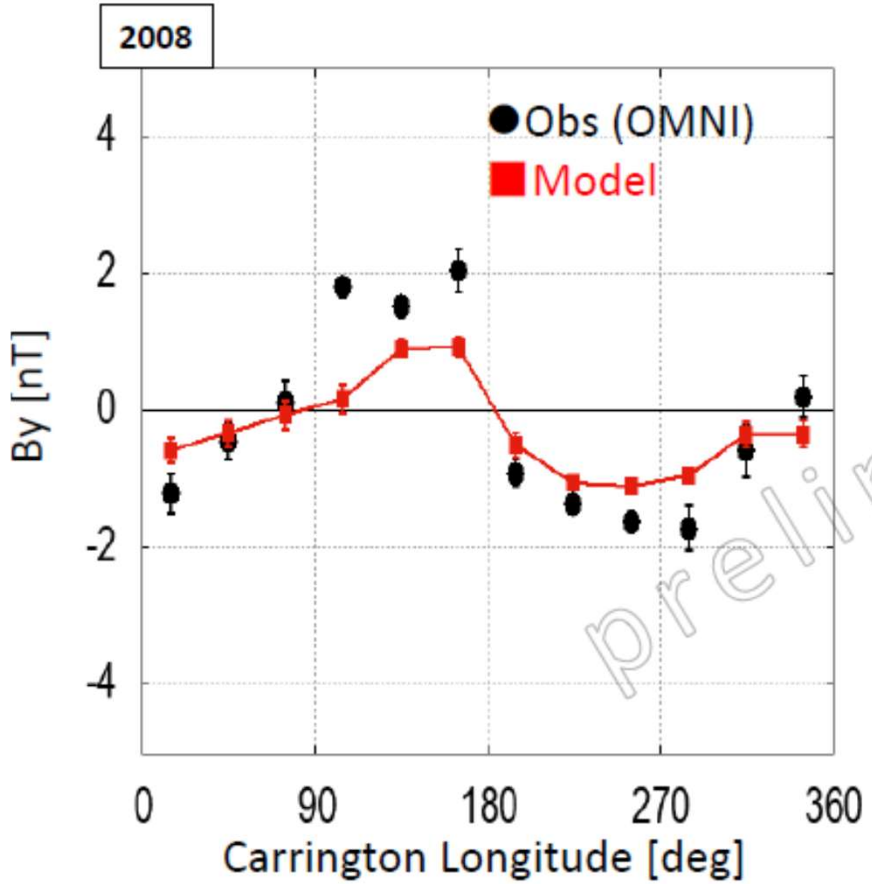

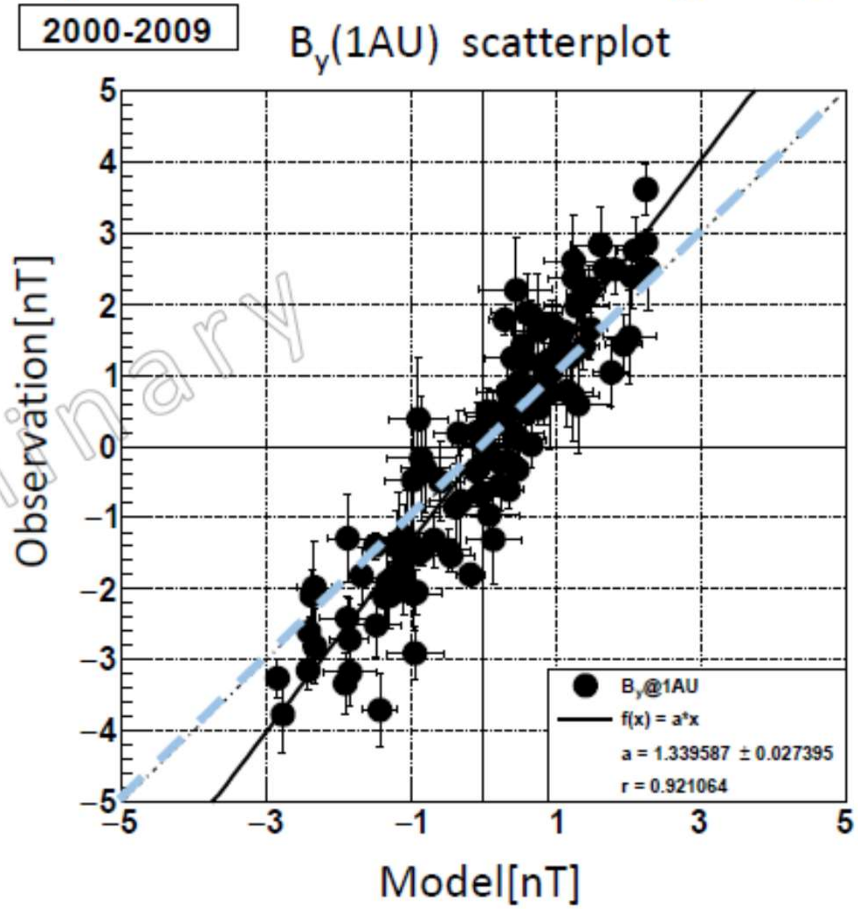

- **The model underestimates IMF strength @1AU (B_{IMF})!**
- **The regression coefficients (B_{obs} / B_{model}), are comparable to the underestimation of α**

1.32 ± 0.04 in Away sector

1.36 ± 0.04 in Toward sector

Discussions

- The solar magnetic field model underestimates N-S displacement observed by Tibet-III, by underestimating the IMF strength
- Possible sources of this underestimation
  - ◆ underestimation of photospheric magnetic field ?
    - photospheric field strength observed by MDI is 1.80 ± 0.20 times larger than Kitt peak used in our simulations (Riley *et. al.* 2014)
    - => But, the underestimation of α is not improved in simulations even with MDI
  - ◆ refinement of the coronal magnetic field model needed? <= more likely

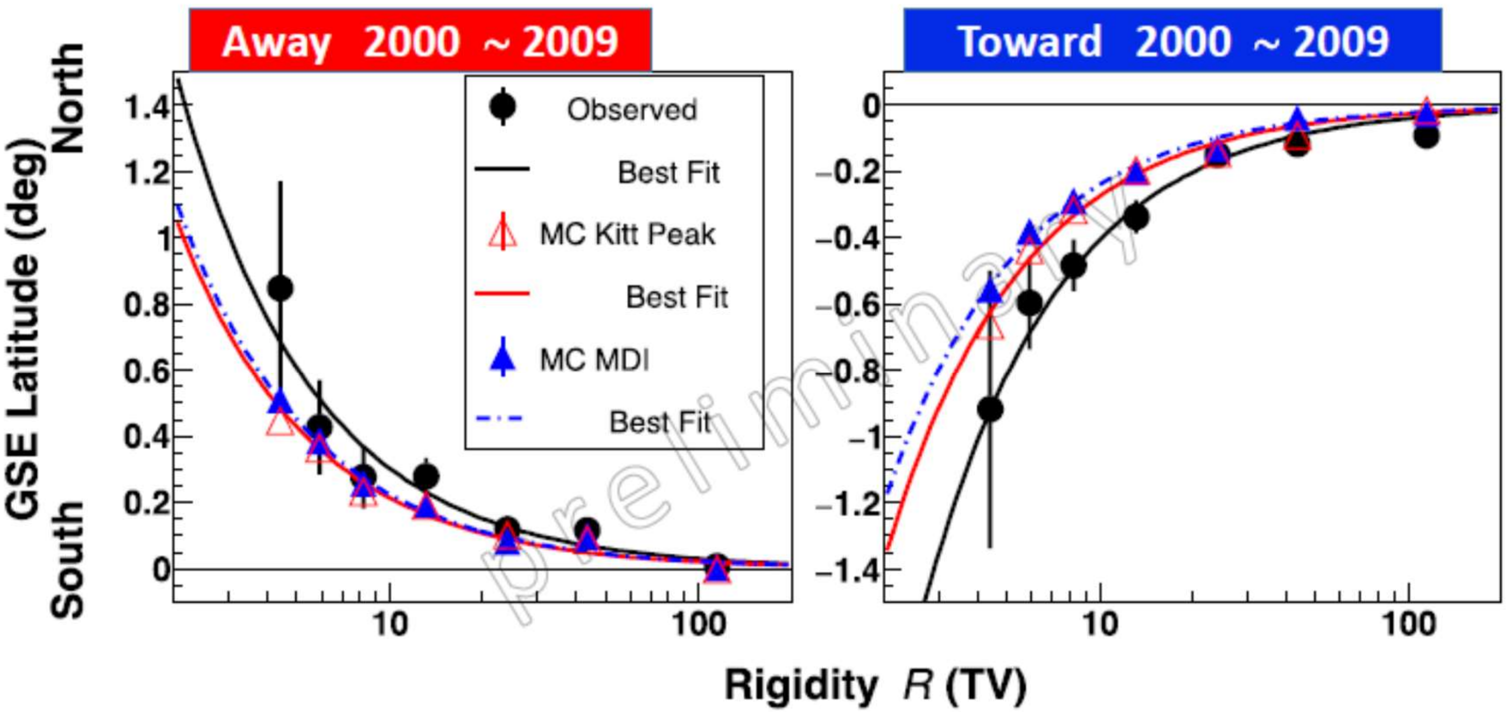

Summary

- MC simulation developed to reproduce the temporal variation of the Sun shadow based on the source surface model (CSSS).

- Comparison between Obs./MC deficit at 3TeV
  - CSSS model apparently fails at the solar maximum.
    - ➢ After the ICME periods are excluded, CSSS better reproduces the observation

- N-S displacement of the Sun shadow observed:

  $1.54 \pm 0.21_{stat} \pm 0.20_{sys}$ $(1.62 \pm 0.15_{stat} \pm 0.22_{sys})$ x

  the prediction in Away (Toward) sector.
    - ➢ Implication that our simulation underestimates average IMF strength.

  (Refinement of CSSS model may be needed,

  while Parker model should be OK!)

- **Complementary to satellite observations, ground-based cosmic-ray experiments can contribute to solar magnetic field measurements !**